Manuscript Details

Manuscript number	MEMSCI_2017_66
Title	Understanding the Effect of Zeolite Crystal Expansion/Contraction on Separation Performance of NaA Zeolite Membrane: A Combined Experimental and Molecular Simulation Study
Article type	Full Length Article

Abstract

Experimental measurements and molecular simulations were used to understand the effect of adsorption-induced changes in zeolite crystal size on the separation performance of NaA zeolite membrane for dehydration of alcohols. The vapor permeation (VP) separations of water/ IPA showed a dramatic increase of IPA flux as the feed water concentration decreased. However, in the case of water/methanol and water/ethanol mixtures, the alcohol fluxes were almost independent of the feed water concentration. Permporosimetry measurements as well as molecular simulations show that at low loading of water, NaA crystals contract slightly, while they expand at higher loadings. Both methanol and ethanol can enter the zeolite to reduce the crystal contraction. However, isopropanol cannot enter the NaA crystal and is thus unable to mitigate the effects of low water loadings. Based on this knowledge, the presence of methanol or ethanol in the water/isopropanol mixtures with low water content was expected to improve the dehydration performance of NaA zeolite membrane. This result was also observed for the dehydration of water/other large molecular mixture. Our studies here provide an improved understanding of the permeation and separations for NaA zeolite membrane.

Keywords	NaA zeolite membrane; dehydration; alcohol; structural change, defect
Manuscript category	Inorganic Membranes

Corresponding Author	Xuehong Gu
Corresponding Author's Institution	Nanjing Tech University
Order of Authors	Fanyu Qu, Rui Shi, Li Peng, Yuting Zhang, Xuehong Gu, Xiaoyu Wang, Sohail Murad
Suggested reviewers	Freek Kapteijn, Mikel Duke, Yushan Yan, Junhang Dong, Zhengbao Wang

Submission Files Included in this PDF

File Name [File Type]

Cover Letter.docx [Cover Letter]

Manuscript.docx [Manuscript File]

Fig.1.tif [Figure]

Fig.2.tif [Figure]

Fig.3a.tif [Figure]

Fig.3b.tif [Figure]

Fig.3c.tif [Figure]

Fig.3d.tif [Figure]

Fig.4a.tif [Figure]

Fig.4b.tif [Figure]

Fig.5a.tif [Figure]

Fig.5b.tif [Figure]

Fig.6.tif [Figure]

Fig.7a.tif [Figure]

Fig.7b.tif [Figure]

Fig.7c.tif [Figure]

Fig.7d.tif [Figure]

Fig.7e.tif [Figure]

Fig.7f.tif [Figure]

Fig.8a.tif [Figure]

Fig.8b.tif [Figure]

Fig.9a.tif [Figure]

Fig.9b.tif [Figure]

Fig.10a.tif [Figure]

Fig.10b.tif [Figure]

Fig.11a.tif [Figure]

Fig.11b.tif [Figure]

Fig.12a.tif [Figure]

Fig.12b.tif [Figure]

Highlights.docx [Highlights]

To view all the submission files, including those not included in the PDF, click on the manuscript title on your EVISE Homepage, then click 'Download zip file'.

Dear Editor,

We are pleased to submit a paper entitled "**Understanding the Effect of Zeolite Crystal Expansion/Contraction on Separation Performance of NaA Zeolite Membrane: A Combined Experimental and Molecular Simulation Study**" (by Fanyu Qu, Rui Shi, Li Peng, Yuting Zhang, Xuehong Gu*, Xiaoyu Wang, Sohail Murad) to be considered for publication in ***Journal of Membrane Science*** as an original papers.

NaA zeolite membranes have been commercially applied in dehydration of organics. We realized that separation performance of NaA zeolite membranes was strongly related with specific separation systems in practical applications. Due to multicrystalline structure of NaA zeolite membrane, the intercrystalline pores changed by expansion/contraction of zeolite crystals in separation systems make a great effect on membrane separation performance. In this paper, both experimental and molecular simulation studies were systematically carried out to understand such an effect on separation performance of NaA zeolite membrane. We believe the achieved results would be helpful for further development of use of NaA zeolite membranes in industrial separations.

The work has not been submitted elsewhere for publication, in whole or in part, and all the authors listed have approved the manuscript that is enclosed.

I look forward to hearing from you on the status of this manuscript. Thank you very much for your consideration.

Best regards,

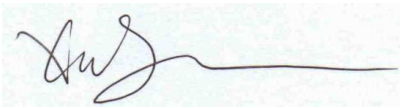

Xuehong Gu
Professor of Chemical Engineering
State Key Laboratory of Materials-Oriented Chemical Engineering
College of Chemical Engineering
Nanjing Tech University
Nanjing 210009, P. R. China
Tel.: +86-25-8317-2268
E-mail: Xuehonggu@yahoo.com

Understanding the Effect of Zeolite Crystal Expansion/Contraction on Separation Performance of NaA Zeolite Membrane: A Combined Experimental and Molecular Simulation Study

Fanyu Qu[1], Rui Shi[1], Li Peng[1], Yuting Zhang[1], Xuehong Gu[1,*], Xiaoyu Wang[2], Sohail Murad[2]

[1] State Key Laboratory of Materials-Oriented Chemical Engineering, College of Chemical Engineering, Jiangsu National Synergetic Innovation Center for Advanced Materials, Nanjing Tech University, 5 Xinmofan Road, Nanjing 210009, PR China

[2] Department of Chemical and Biological Engineering, Illinois Institute of Technology, Chicago, Illinois 60616, USA

***Corresponding author: Prof. Xuehong Gu**

Tel.: +86-25-83172268; Fax: +86-25-83172268

E-mail: Xuehonggu@yahoo.com

Abstract

Experimental measurements and molecular simulations were used to understand the effect of adsorption-induced changes in zeolite crystal size on the separation performance of NaA zeolite membrane for dehydration of alcohols. The vapor permeation (VP) separations of water/IPA showed a dramatic increase of IPA flux as the feed water concentration decreased. However, in the case of water/methanol and water/ethanol mixtures, the alcohol fluxes were almost independent of the feed water concentration. Permporosimetry measurements as well as molecular simulations show that at low loading of water, NaA crystals contract slightly, while they expand at higher loadings. Both methanol and ethanol can enter the zeolite to reduce the crystal contraction. However, isopropanol cannot enter the NaA crystal and is thus unable to mitigate the effects of low water loadings. Based on this knowledge, the presence of methanol or ethanol in the water/isopropanol mixtures with low water content was expected to improve the dehydration performance of NaA zeolite membrane. This result was also observed for the dehydration of water/other large molecular mixture. Our studies here provide an improved understanding of the permeation and separations for NaA zeolite membrane.

Keywords: NaA zeolite membrane; dehydration; alcohol; structural change, defect

1. Introduction

Dense zeolite membranes demonstrate high separation selectivity for molecular separations based on their well-defined micropores and preferential adsorption property. However, because of the multicrystalline structure of zeolite membranes, the separation performance is strongly affected by intercrystalline defects. These intercrystalline nonzeolitic pores are mostly larger than zeolite pores resulting in lower separation selectivity. NaA zeolite membranes with LTA structure are commonly used for dehydration of solvents because of their strong hydrophilicity and suitable pore size [1-5]. Even in the presence of nanometer-sized defects, a high pervaporation selectivity up to 10000 has been achieved using the NaA membranes [6-9]. Capillary condensation is generally used to explain the phenomenon, where water molecules are adsorbed in the defects and block the flow of other (larger) molecules through them [8, 9].

Recently, we found that the isopropanol (IPA) flux through NaA membrane increased rapidly as the concentration of water decreased in the water/IPA mixture during vapor permeation (VP). However, such behavior was not observed in the case of water/ methanol or water/ ethanol mixture. Shah et al. also found similar behavior for NaA membranes during their study on the permeation fluxes of pure components through zeolite membrane [10]. The IPA flux was more than three times the ethanol flux and slightly higher than the methanol flux. While capillary condensation may explain the observed increase in IPA flux through NaA membranes as water content decreasing, it cannot explain the relatively stable flux of methanol or ethanol as water

content decreases. Since IPA (kinetic diameter ~0.48 nm) is larger than the zeolite A pores (0.42 nm), it only enters and subsequently transports through the defects. Meanwhile, methanol (0.38 nm) and ethanol (0.43 nm) can enter both the NaA zeolite pores and the defects, thus the methanol or ethanol flux should also increase largely according to capillary condensation mechanism. Although the observed behavior is essentially attributed to preferential adsorption, a more reasonable explanation could be that there are changes in the effective size of the defects due to such adsorption, as well as changes in the crystal sizes.

A series of extensive studies on MFI zeolite membranes by Noble and Falconer demonstrated that polycrystalline zeolite membranes are flexible and defect sizes can decrease or increase when certain molecules adsorb in the zeolite pores [11-18]. For example, they found the molecules with sizes larger than MFI pores, such as DMB and 1,3,5-trimethylbenzene (TMB), showed fluxes through MFI zeolite membrane as high as 2 orders of magnitude larger than those for n-hexane during single-component pervaporation, although n-hexane is significantly smaller than these molecules. The low n-hexane flux was attributed to the decrease of the size of defects induced by MFI crystal expansion upon n-hexane adsorption [11]. X-ray diffraction measurements [12] further confirmed that MFI crystals expanded upon n-hexane adsorption. Feeding small amounts of gases or vapors that expand zeolite unit cell size reduce permeation through nonzeolitic pores [13-17]. This effect was so pronounced that in some cases, it significantly enhanced permselectivity [16, 17]. On the other hand, a negative impact on permselectivity was also observed due to adsorption of compounds at

certain loadings that shrink the MFI zeolite size (i.e. *p*-xylene, *i*-butane, etc.) [18].

Adsorption induced changes of NaA zeolite crystal unit cell size has been previously reported [19-22]. Adsorption of water may cause both shrinkage and swelling of the NaA zeolite crystals. Sarakhov et al. [19] reported that the NaA unit cell contracted as much as 0.3 vol.% at 295 K due to adsorption at low loadings of water and expanded 0.57 vol.% at higher saturation water loadings. Caro et al. [20] studied the change of the unit cell dimension for zeolites as a function of temperature and water content by in situ-heating XRD. A significant change was observed in LTA type zeolites because of de-watering. They also attributed the difficulty in preparation of shape-selective LTA membranes for gas separations to the extreme expansions/shrinkages of its unit cell during water removal [21]. Sorenson et al. [22] found that at a thermodynamic activity of 0.03 water contracted NaA zeolite by 0.22 vol.% and increased helium flux through a NaA membrane by about 80%; it also increased the *i*-butane flux by 14% during vapor permeation and *i*-propanol flux by 25% during pervaporation. At activities above 0.07, water expanded NaA crystals and they observed decreases in the fluxes of helium, *i*-butane, and IPA through the NaA membrane. They concluded that the observed high pervaporation selectivities for water/alcohol separations in zeolite NaA membranes were due, at least partially, to water-induced expansion of NaA crystals.

All these previous studies have shown that zeolite membranes are flexible and the size of the inter-crystalline non-zeolite pores can change due to adsorption of suitable molecules. However, the effect of the adsorption induced changes in NaA

crystals on the membrane separation performance has not been widely studied. Since NaA membranes are widely used to dehydrate solvents in industrial applications, a better understanding of this phenomenon will be valuable for improving these processes. Molecular simulation studies since the 1990s have traditionally used flexible models to study zeolites [23]. In our studies, we have also used a flexible zeolite framework model to examine the contractions/expansion of the framework.

In this paper, we have investigated the water and alcohol adsorption in NaA crystals and the resulting crystal swelling or shrinkage and their effect on selectivities of NaA membranes for alcohol/water mixtures separation by vapor permeation. Tubular NaA zeolite membranes were used in this study and the membrane separation performance (flux and selectivity) of various binary water/alcohol (water/methanol, water/ethanol, water/isopropanol) mixtures over a range of water concentration between 0.5 to 5 wt.% at 373 K were investigated. Four unit cells of the zeolite was investigated to simulate the changes in the NaA unit cell size induced by adsorption and permporosimetry measurements were used to determine the corresponding changes in the size of the defects. We believe the observed permeation results can be explained by the changes in size of the defects in the zeolite membrane due to adsorption. These conclusions are based on both our molecular simulations as well as permporosimetry studies. To further reinforce out conclusions we carried out additional studies with ternary mixtures which further confirmed our results and observations.

2. Experimental

2.1 Preparation of NaA zeolite membrane

NaA zeolite membranes were supplied by Jiangsu Nine Heaven High-Tech Co., Ltd. The membranes were hydrothermally synthesized on a porous mullite tube using the secondary growth method as described in our previous work [24]. The support had a length of 80 cm, an outer diameter of 12 mm, a wall thickness of 2.5 mm, a porosity of ~40% and an average pore size of 1 μm. The outer surface of the support was coated with NaA zeolite seeds before membrane synthesis. The seeded support was then immersed in a synthesis gel loaded in an autoclave. The synthesis solution was prepared by dissolving sodium aluminate, water glass and sodium hydroxide in deionized water at room temperature. All the chemicals used were industrial grade from commercial companies in China. The molar composition of synthesis gel was $A1_2O_3$: SiO_2: Na_2O: H_2O=1:2:2:120. Hydrothermal synthesis was carried out at 373 K for 4 h. The as-synthesized membrane was cut into 70 mm in length and washed withdeionized water and dried in an oven overnight before pervaporation (PV) and vapor permeation (VP) tests. The morphologies of NaA zeolite membranes were observed by Field Emission Scanning Electron Microscopy (FE-SEM, S-4800, Hitachi). The crystal phases were determined by X-ray diffraction (MiniFlex 600, Rigaku) with Cu Kα radiation in the 2θ rang of 5-50°.

2.2 Pervaporation and vapor permeation tests

PV performance of NaA zeolite membranes was evaluated using 90 wt.% ethanol/water mixtures at 383 K which was reported in our previous work [24]. VP

performance of tubular NaA zeolite membranes was investigated by dehydration of binary methanol/water, ethanol/water, IPA/water mixtures and ternary IPA/ethanol/water and IPA/methanol/water mixtures. Fig. 1 shows a schematic diagram of VP apparatus for evaluating a membrane. The tested membrane had an effective membrane area of ca. 15.8 cm^2. Feed steam was continuously pumped into the shell side of a membrane module by steam pressure at 0.1-0.4 MPa and the permeate was removed from the lumen by a vacuum pump, which maintained a downstream pressure below 200 Pa. The permeated vapor was collected with a cold trap cooled by liquid nitrogen. Both of the samples at the feed and permeate sides were analyzed by a gas chromatography (GC-2014A, Shimadzu) equipped with a thermal conductivity detector and a packed column of Parapak-Q. The membrane performance was determined by permeation flux (J) and separation factor (α), which were respectively defined as follows:

$$J = m / (A \cdot t) \tag{1}$$

$$\alpha_{i/j} = \frac{y_i / y_j}{x_i / x_j} \tag{2}$$

Where m is the total mass of the permeate product, kg; A is the effective area of the membrane, m^2, t is the elapsed time, h; y_i/y_j is the weight fraction ratio of water over alcohol in the permeate and x_i/x_j is the corresponding ratio in the feed.

2.3 Permporosimetry measurement

Permporosimetry was used to evaluate membrane quality by measuring helium flow through the membrane. The test system was described in a previous publication

[25]. Prior to permporosimetry test, the membrane mounted in a permeator was heated at 383 K for 24 h in a flowing helium stream to remove any adsorbate in zeolitic and nonzeolitic pores. The operating temperature was then fixed at 313 K for permporosimetry experiment. Dried helium was used as a non-condensable gas and absorbate vapor was employed as a condensable gas. Water or a high purity alcohol (methanol, ethanol and isopropanol) (AR) mixed with a small amount of CaO was loaded in a saturator for producing absorbate vapor. The feed stream was obtained by mixing a pure helium stream with another helium stream saturated with the absorbate. The absorbate activity (the ratio of absorbate partial vapor pressure to its saturation pressure P/P_{sat}) was varied by adjusting the ratio of the two helium flows. The feed pressure was maintained at 201 and 121 kPa and the permeate pressure was kept at atmospheric pressure (101 kPa).

2.4 Molecular simulations

2.4.1. Potential Models

The framework for NaA zeolite was obtained from the database IZA-SC (Structure Commission of the International Zeolite Association) [26]. The potential parameters for the zeolite are based on our previous studies, which showed good agreement for water adsorbed in the zeolite framework [27]. We would like to note in our model the framework atoms are tethered to their equilibrium site (to allow for flexibility of the zeolite framework) with a suitable harmonic constant [28]. The potential models for water and isopropanol alcohol (IPA) are based on the AMBER

force field [29], and have the following functional form:

$$E_{total} = \sum_{bonds} K_b(\mathrm{b}-\mathrm{b}_{\mathrm{eq}})^2 + \sum_{angles} K_\theta(\theta-\theta_{\mathrm{eq}})^2 + \sum_{dihedrals} \frac{V_n}{2}\left[1+\cos\left(n\phi-\gamma\right)\right] + \sum_{i<j}\left[\frac{A_{ij}}{R_{ij}^{12}} - \frac{B_{ij}}{R_{ij}^{6}} + \frac{q_i q_j}{\varepsilon R_{ij}}\right] \quad (3)$$

The potential model has intramolecular and intermolecular contributions. The first three terms represent bond lengths, bond angles and dihedral angles. The forth term describes the intermolecular contributions using Lenard-Jones 12-6 potentials and classic coulombic interactions. We used 14 Å cut off for LJ interactions, while Ewald methodology was used for long range electrostatic interactions [30].

2.4.2. System set up

The schematic diagram of the system simulated is shown in Fig. 2 and is based on our previous studies for similar systems [31]. The central (middle) compartment of simulation box contains the vapor phase being investigated. Two layers of NaA zeolite membranes separate this section from the two side compartments which are initially empty (vacuum) to provide the driving force for the vapors to permeate the zeolite membranes. Two systems were investigated. The first system contains only pure IPA in the vapor phase while the second system consists of IPA containing 5 wt.% by weight water. The system size was chosen to ensure that no vapor condensation takes place in the bulk phase of the vapor compartment at the system temperature of 423 K. A simulated defect was created by removing some framework molecules around a chosen pore to make the defect size roughly 12 Å.

2.4.3. Simulation details

All simulations are carried out under non-equilibrium conditions using the LAMMPS simulation package [32]. Energy minimization was performed using the Polak-Ribiere conjugate gradient method and the Verlet algorithm was used to carry out the time integration. The system volume was kept without change and a Nosé-Hoover thermostat (with a damping constant of 100 fs) was applied to the solution and membrane atoms throughout the simulation in order to maintain a constant temperature of 423 K. Following minimization, a timestep of 1.0 fs was used for production runs of 5,000,000 steps (5 ns).

3. Results and Discussion

3.1. Membrane characterizations

Fig. 3 shows the morphologies of as-synthesized NaA zeolite membranes. As can be seen, for both M1 and M2, the support surfaces were completely covered by cubic crystals with well intergrowth. No cavity between the crystal particles was found by SEM. The membranes were approximately 20 μm thick. Pervaporation of a 10 wt.% water/ethanol mixture at 348 K showed selectivities greater than 5000 for membranes M1 and M2 (Table 1), indicating they were both high quality membranes. Both water flux and water separation factor of M2 were higher than those for M1, indicating less defects existed in M2.

3.2 Separation of binary mixture

Fig. 4 shows water flux and separation factor of NaA zeolite membrane M1 as a

function of feed water content in VP separations of water/methanol, water/ethanol and water/IPA binary solutions at 373 K. The water permeation fluxes in all above systems decreased when the water content decreased, which was resulted from the decreasing driving force. The ethanol and methanol fluxes were almost stable, and remained below 0.005 and 0.05 kg m^{-2} h^{-1}, respectively. The corresponding separation factors for the both solutions stayed above 10000 and 200 at feed water content 0.5-5 wt.%. However, the IPA flux increased significantly from 0.2 to 2.5 kg m^{-2} h^{-1} as water content declined from 5 to 0.5 wt.%, resulting in low separation performance at low water content. As shown in Fig. 4b, the separation factor for water over IPA dropped from 150 to 15 accordingly. The results indicated that the separation performance of NaA zeolite membrane was strongly related with separation system. Even though IPA has a larger molecular size, we were unable to obtain high separation selectivity (as compared with ethanol solution).

It was not clear whether the change of IPA flux was related with the number of defects embedded in zeolite layer. Therefore, the separation of binary water/alcohol mixtures was also evaluated with zeolite membrane M2 (which is higher quality as mentioned earlier). The VP separation results at 373 K are shown in Fig. 5. In general, M2 showed better VP separation performance for binary water/alcohol mixtures compared to M1. These results were consistent with pervaporation separation results, indicating that M2 was of a higher quality (fewer defects). Interestingly, similar trends were observed over M2 for water and alcohol fluxes with changes in water content in feed. As the water content in feed mixture decreased, IPA flux increased gradually,

while ethanol and methanol fluxes were relatively unchanged. As shown in Fig. 5a, IPA flux increased from 0.01 to 0.18 kg m^{-2} h^{-1} as water content decreased from 5 to 0.2 wt.%. Obviously, the change of IPA flux over M2 was less than that over M1.

The increased IPA flux with reduction of water content in the feed was observed in both higher quality membrane M2 and the relatively lower quality membrane M1. IPA, with a kinetic diameter of 0.48 nm, is too large to either enter or adsorb in the LTA zeolitic pores at the temperatures used, and thus it must diffuse/permeate through nonzeolitic pores (defects) in the membrane. It is well known that, the size of NaA zeolite crystal can change when certain molecules are adsorbed in pores, and these can lead to changes in the size of the defects in the zeolite membrane [19, 22]. The dramatic increase of IPA flux resulted from an increase of inter-crystal pass path which was probably caused by the shrinkage of NaA zeolite crystals at low water loading. Obviously, these adsorption induced changes in the NaA zeolite crystal size will not have any significant impact on the performance of zeolite membrane with less intercrystalline defects. This also explains why relatively smaller changes in the IPA flux were observed in M2 compared to M1 (0.01 to 0.18 kg m^{-2} h^{-1} *vs*. 0.2 to 2.5 kg m^{-2} h^{-1}). In case of methanol and ethanol, their kinetic diameters (0.38 nm and 0.43 nm, respectively) are smaller than or similar to the size of LTA pores. They then can enter and adsorb in the zeolite pores when water loadings is low even though the LTA zeolite pores do exhibit preferential water adsorption. As a result, the shrinkage of NaA zeolite crystals at low water loading and the resulting increase of defect size is not observed. This also explains the relatively unchanged alcohol flux observed

through NaA zeolite membrane for the water/methanol and water/ethanol binary mixture regardless the water content in the feed.

We also used molecular simulations to get a molecular level understanding of the behavior observed experimentally. Our simulation results, as shown in Fig. 6, confirm the experimentally observed behavior. However, as will be discussed below the simulations also provided significant insight into why this unusual phenomenon occurs. Simulations were carried out for pure IPA, and 5 and 10% by weight water in the IPA. As can be seen clearly, the IPA was able to permeate the defect quite readily in the absence of water. Once water was introduced the IPA permeation was essentially stopped. Our simulations indicated there were two primary reasons why the IPA permeation was prevented when water is present. Firstly, the water molecules get adsorbed in zeolite pores and defects thus essentially reducing the effective size of the defects. With water present at the defect sites, IPA molecules also get adsorbed with a high adsorption energy which effectively blocks the defect. In addition, in our simulations we observed another interesting phenomenon. In the bulk vapor phase when water is presented the IPA molecules tend to form IPA clusters which also effectively increases the size of the IPA molecules and thus increases their dynamic diameter making it more difficult for them to permeate the zeolite defects. This is clearly shown in Fig. 7 and Fig. 8.

3.3 Influence of absorbate water on expansion/contraction in NaA zeolite crystal

To evaluate the influence of absorbate water molecule on expansion/contraction in NaA zeolite crystal, a permporosimetry measurement was further conducted on

NaA zeolite membrane. Fig. 9 shows permporosimetry results of NaA zeolite membrane under different water feed pressures of 20 and 100 kPa. As shown in the figure, the dependence of helium permeance on water activity at 20 kPa was similar to that at 100 kPa, indicating that no capillary condensation occurred under lower feed pressure. It was also suggested that viscous flow was not involved in helium permeation due to relatively small size of intercrystalline pores. The variation in helium permeance was mainly due to the enlargement and shrinkage of membrane defects. At low water activity below 0.3, the helium permeance was higher than the initial one, representing the enlargement of membrane defects caused by contraction of NaA zeolite crystals. The highest helium permeance as related to the maximum contraction of zeolite unit cell was observed at the water activity of 0.07 when the feed pressure was 20 kPa. As water activity was further increased, the helium permeance declined instead, representing the shrinkage of membrane defects resulted by expansion of NaA zeolite crystals. The phenomenon was in accordance with the observation by Sorenson et al [13]. At high water activity, the helium permeance approached to zero and decreased very slightly, implying that most of membrane defects had been closed at that time.

Permporosimetry measurements were further conducted on the same membrane by using methanol, ethanol and IPA as absorbates respectively. As shown in Fig. 10, similar contraction/expansion behaviors of NaA zeolite crystals were also seen by using IPA as absorbate. As we know, IPA molecules have large kinetic diameters (IPA: 0.48 nm) that cannot allow them to enter the NaA zeolitic pores. The initial

increase in helium permeance could be attributed to the trace concentration of water in IPA in spite of an effort to remove it by adding CaO powders into anhydrate IPA. Without addition of CaO powders into anhydrate IPA, a significant increase in helium permeance could be observed (not shown in Fig. 9). The further decline in helium permeance with increase of IPA activity was mainly due to the blocking resulting from IPA adsorption on membrane defects. In the case of ethanol, a similar trend was observed but the initial increase in helium permeance was smaller compared to when IPA was present. Besides, the decline of helium permeance after the increase was only slight. As discussed above, although kinetic diameter of ethanol is similar to NaA zeolite pore size, a small amount of ethanol molecules can enter into the zeolitic pores, which could compensate for the contraction of NaA zeolite caused by water adsorption. The increase of ethanol activity could result in expansion of zeolite crystals and thus reduce helium permeation. Due to the formation of IPA clusters, more defects could be blocked at high activity. As a result, the final helium permeance for IPA was lower than that for ethanol. For methanol as absorbate, the expansion effect is significant as the molecules can more readily absorb into the NaA zeolite pores. Therefore, the helium permeance decreased continuously with its activity.

Results from molecular simulations also show that at low water loadings the zeolite framework tends to contract but as the water loading increases the framework tends to expand. When water loading is low it tends to accumulate in the center of the zeolite cavity and consequently framework sites because of the strongly polar nature

of the water molecules are attracted towards the center. As the water loading increases they start occupying areas near the framework atoms, and repulsive forces then tend to push the framework molecules out which leads to an expansion of the framework. We would like to point out that the changes in both experiments and simulations generally are in agreement. Although the changes are relatively small, the as-caused changes in defect size could be significant. The complete results are shown in the Table 2.

3.4 Effect of defects size change in dehydration of complex solvent mixture

Most laboratory studies have investigated unary and binary pervaporation or vapor permeation. However, separation of multicomponent feed often occurs in industrial processes. For example, pharmaceutical streams are complex mixtures of various solvents. In many cases, these mixtures form binary/ternary azeotropes due to presence of water, hindering the recovery of valuable solvents. In such cases, using a hydrophilic zeolite membrane to remove water from the mixture by pervaporation or vapor permeation can be effectively used to break the azeotrope (with significantly lower energy requirements) and the solvent mixture can be further purified by distillation. The separation of such streams containing IPA, methanol or ethanol and water were studied here. As pointed out earlier, methanol and ethanol adsorption can swell the LTA crystals and this can lead to a decrease in the size of the non-zeolitic pores. This would then lead to a decrease in the flux of IPA, since it only diffuses through non-zeolitic pores.

Fig. 10 shows the improved separation performance of NaA zeolite membrane

M1 as a function of water content when 6 wt.% methanol or ethanol was added into the feed at 373 K. The IPA flux decreased dramatically after methanol or ethanol was added to the feed (Fig. 10a). In addition, no obvious changes in the fluxes in both ternary mixtures were observed when the water content in the feed was increased above 1.5 wt.% (Fig. 10b). We believe the following explanation rationalizes this observation. In ternary mixtures, the permeation of IPA is hindered by the presence of methanol or ethanol in the following manner. Molecules with relatively small molecular size and high hydrophilicity (such as methanol and ethanol) can diffuse and adsorb both in the pores of hydrophilic NaA zeolite membrane as well as any defects that exist. It was observed that the IPA flux significantly increased as the water content decreased below 1.5wt.% in the water/IPA/ethanol ternary system. For example, the IPA flux for 0.5 wt.% water in the feed was double the IPA flux value for 1.5 wt.% water in the feed. The selectivity also decreased from 200 to 80. Meanwhile, the IPA flux in the water/IPA/methanol ternary system was relatively unchanged, and the selectivity stayed above 300. This behavior resulted both from contraction and expansion of the NaA zeolite crystal by adsorption of smaller molecules in the zeolitic pores, which effectively decreases the defect size and prevents IPA from diffusing through these defects. This behavior is explained in more detail below.

The permporosimetry measurements show that as the water concentration decreased from 1.5 to 0.5 wt.% (from 0.17 to 0.06 activity), the crystal contracted. However, since both methanol and ethanol can also adsorb in NaA pores, this then led

to expanding the crystal at the concentration of 6 wt.% thus neutralizing the contraction at otherwise low water concentration. In addition, the methanol also adsorbs on the defect sites and effectively decreases the size of the defects significantly. Although the exact nature of crystal change may be different when both water and alcohol adsorb in NaA pores, overall similar behavior is observed and expected. The adsorption of ethanol will also cause crystal expansion to partly compensate the crystal contraction at low water content. However, since ethanol is larger in size and less polar it does not completely neutralize the effects of low water loading. In addition, because of its weaker polarity, it does not adsorb as strongly on the defects and does not reduce the defect as significantly as methanol (or water). Thus, the IPA flux increased as the water content decreased from 1.5 to 0.5wt.%, but lower than that of binary system. With methanol, the behavior was similar to that of high water loading.

The dependence of IPA flux on the methanol or ethanol concentration in the feed (Fig. 11) showed that, with addition of methanol or ethanol (>10 wt.%), the IPA flux significantly decreased by about 30% or 10% of the value in binary water/ IPA mixture. The possible reason for the decrease of IPA permeation fluxes is the decreasing driving force caused by the decreasing IPA content with the increase of smaller alcohol concentration. The IPA fluxes decreased slightly with further increases in concentration to about 20 wt.%, after which they stay essentially unchanged. Interestingly, water/IPA selectivity increased with the increase of methanol or ethanol concentration below 20 wt.%. The results suggested that

expansion of NaA zeolite crystals induced by adsorption of smaller alcohols was sensitive to the concentration of smaller alcohols contained. Further increase in methanol or ethanol concentration did not change water/IPA selectivity significantly, indicating a saturated adsorption of smaller alcohols in zeolitic pores. For the water/IPA mixture, NaA zeolite membrane showed better separation performance with methanol included as the ternary component in the feed due to larger adsorption of methanol in the zeolitic pores as results in increased crystal expansion.

The separation performance of NaA zeolite membrane for the mixture of water and other larger molecules, such as *n*-butanol, which only diffuse through non-zeolitic pores (defects), demonstrated similar behavior as shown in Fig. 12. The fluxes of butanol decreased with existence of methanol or ethanol, but did not show obvious difference as the case of IPA. This is because butanol like IPA is unable to diffuse into the zeolitic pores, and is less polar to adsorb in both the pores and the defects sites. The kinetic diameter of butanol is 0.463 nm [33], which is larger than the pore size of NaA zeolite (0.42 nm) and almost comparable to the diameter of IPA (0.48 nm).

4. Conclusion

In this work, the effect of adsorption-induced changes in zeolite crystal size on the separation performance of NaA zeolite membrane for dehydration of alcohols was investigated using experimental measurements in combination with molecular simulations. Experiments were conducted with various water/alcohol (water/methanol,

water/ethanol, water/isopropanol) mixtures over a range of water concentration between 0.5 to 5 wt.% at 373 K with tubular NaA zeolite membranes. The alcohol fluxes and the corresponding separation factors for water/methanol and water/ethanol mixtures were found to be almost independent of the feed water concentration. However, for water/isopropanol mixture, we observed a dramatic increase in the IPA flux and a corresponding decrease in the water/isopropanol separation factor as the feed water concentration decreased. Permporosimetry measurements as well as molecular simulations show that at low loading of water NaA crystals contract slightly, while they expand similarly at higher loadings. In addition, defects in crystal do not attract enough adsorbed water molecules to block the defects, which leads to a high resulting flux and lower separation factors. However, if methanol and ethanol are present in the mixture, they enter the zeolite and thus both reduce the crystal contraction and block the defects by adsorbing at the defect sites. This then prevents high IPA flux and the loss in separation factors observed. Unlike methanol or ethanol, isopropanol cannot enter the NaA crystal and is thus unable to mitigate the effects of low water loadings. Thus an increase of the isopropanol flux can be observed as the decrease of feed water concentration. Based on this knowledge, the presence of methanol or ethanol in the water/isopropanol mixtures with low water content can be expected to improve the dehydration performance of NaA zeolite membrane. Our studies have enabled us to provide an improved understanding of changes in the sizes of zeolite crystals effects on NaA zeolite membrane permeation and separations, which will enable further development of use of NaA zeolite membranes in industrial

separations.

Acknowledgement

This work is sponsored by the National Natural Science Foundation of China (21222602, 21490585), National High-tech R&D Program of China (2015AA03A602), the Outstanding Young Fund of Jiangsu Province (BK2012040), Young Fund of Jiangsu Province (BK20130915), the “Six Top Talents” and “333 Talent Project” of Jiangsu Province. XW and SM were additionally supported by grants from the US National Science Foundation (grant no. CBET 1263107/1545560).

Reference

[1] Y. Morigami, M. Kondo, J. Abe, H. Kita, K. Okamoto, The first large-scale pervaporation plant using tubular-type module with zeolite NaA membrane, Sep. Purif. Technol. 25 (2001) 251–260.

[2] T. Gallego-Lizo´n, E. Edwards, G. Lobiundo, L.F. Santos, Dehydration of water/t-butanol mixtures by pervaporation: comparative study of commercially available polymeric, microporous silica and zeolite membranes, J. Membr. Sci. 197 (2002) 309–319.

[3] H. Richter, I. Voigt, J.T. Kuehnert, Dewatering of ethanol by pervaporation and vapour permeation with industrial scale NaA-membranes, Desalination, 199 (2006) 92–93.

[4] Y. Liu, Z. Yang, C. Yu, X. Gu, N. Xu, Effect of seeding methods on growth of NaA zeolite membranes, Micropor. Mesopor. Mater. 143 (2011) 348–356.

[5] Y. Liu, X. Wang, Y. Zhang, Y. He, X. Gu, Scale-up of NaA zeolite membranes on α-Al_2O_3 hollow fibers by a secondary growth method with vacuum seeding, Chin. J. Chem. Eng. 23 (2015) 1114–1122.

[6] J.J. Jafar, P.M. Budd, Separation of alcohol/water mixtures by pervaporation through zeolite A membranes, Micropor. Mesopor. Mater. 12 (1997) 305–311.

[7] M. Kondo, M. Komori, H. Kita, K. Okamoto, Tubular-type pervaporation module with zeolite NaA membrane, J. Membr. Sci. 133 (1997) 133–141.

[8] K. Okamoto, H. Kita, K. Horii, K. Tanaka, M. Kondo, Zeolite NaA membrane: preparation, single-gas permeation, and pervaporation and vapor permeation of

water/organic liquid mixtures, Ind. Eng. Chem. Res. 40 (2001) 163–175.

[9] A.W.C. van den Berg, L. Gora, J.C. Jansen, M. Makkee, T. Maschmeyer, Zeolite A membranes synthesized on a UV-irradiated TiO_2 coated metal support: the high pervaporation performance, J. Membr. Sci. 224 (2003) 29–37.

[10] D. Shah, K. Kissick, A. Ghorpade, R. Hannah, D. Bhattacharyya, Pervaporation of alcohol–water and dimethylformamide–water mixtures using hydrophilic zeolite NaA membranes: mechanisms and experimental results, J. Membr. Sci. 179 (2000) 185–205.

[11] M. Yu, T.J. Amundsen, M. Hong, J.L. Falconer, R.D. Noble, Flexible nanostructure of MFI zeolite membranes .J. Membr. Sci. 182(2007)182– 189.

[12] S.G. Sorenson, J.R. Smyth, M. Kocirik, A. Zikanova, R.D. Noble, J.L. Falconer, Adsorbate-induced expansion of silicalite-1 crystals, Ind. Eng. Chem. Res. 47(2008) 9611–9616.

[13] S.G. Sorenson, E.A. Payzant, R.D. Noble, J.L. Falconer, Influence of crystal expansion/contraction on zeolite membrane permeation, J. Membr. Sci. 357 (2010) 98 –104.

[14] S.G. Sorenson, J.R. Smyth, R.D. Noble, J.L. Falconer, Correlation of crystal lattice expansion and membrane properties for MFI zeolites, Ind. Eng. Chem. Res. 48 (2009) 10021–10024.

[15] J.B. Lee, H.H. Funke, R.D. Noble, J.L. Falconer, High selectivities in defective MFI membranes, J. Membr. Sci. 321 (2008) 309–315.

[16] M.Yu, J.L. Falconer, T.J. Amundsen, M. Hong, R.D. Noble, A controllable

nanometer-sized valve, Adv. Mater. 19 (2007) 3032–3036.

[17] M. Yu, J.L. Falconer, R.D. Noble, Characterizing nonzeolitic-pores in MFI membranes, Ind. Eng. Chem. Res. 47 (2008) 3943–3948.

[18] J.B. Lee, H.H. Funke, R.D. Noble, J.L. Falconer, Adsorption-induced expansion of defects in MFI membranes, J. Membr. Sci. 341 (2009) 238–245.

[19] A.I. Sarakhov, V.F. Kononyuk, M.M. Dubinin, Variation in parameters of crystalline-structure of zeolites during adsorption, Adv. Chem. Ser. 121 (1973) 403–413.

[20] M. Noack, M. Schneider, A. Dittmar, G. Georgi, J. Caro, The change of the unit cell dimension of different zeolite types by heating and its influence on supported membrane layers, Micropor. Mesopor. Mater. 117 (2009) 10–21.

[21] R.M. Barrer, W.M. Meier, Structural and ion sieve properties of a synthetic crystalline exchanger, Trans. Faraday Soc. 54 (1958) 1074–1085.

[22] S.G. Sorenson, E.A. Payzant, W.T. Gibbons, B. Soydas, H. Kita, R.D. Noble, J.L. Falconer, Influence of zeolite crystal expansion/contraction on NaA zeolite membrane separations, J. Membr. Sci. 366 (2011) 413–420.

[23] P. Demontis, E.S. Fois, G.B. Suffritti, S. Quartieri, Molecular Dynamics Studies on Zeolites. 4. Diffusion of Methane in Silicalite, J. Phys. Chem. 94 (1990) 4329–4334.

[24] Z. Yang, Y. Liu, C. Yu, X. Gu, N. Xu, Ball-milled NaA zeolite seeds with submicron size for growth of NaA zeolite membranes, J. Membr. Sci. 392 (2012) 18–28.

[25] Z. Hong, C. Zhang, X. Gu, W. Jin, N. Xu, A simple method for healing nonzeolitic pores of MFI membranes by hydrolysis of silanes, J. Membr. Sci. 366 (2011) 427–435.

[26] Ch. Baerlocher , L.B. McCusker, Database of zeolite structures: http://www.iza-structure.org/databases/

[27] S. Murad, W. Jia, M. Krishnamurthy, Ion-exchange of monovalent and bivalent cations with NaA zeolite membranes: a molecular dynamics study, Molecular Physics, 102 (2004) 2103–2112.

[28] S. Murad, P. Ravi, J.G. Powles, A computer simulation study of fluids in model slit, tubular, and cubic micropores, J. Chem. Phys. 98 (1993) 9771–9781.

[29] W.D. Cornell, P. Cieplak, C.I. Bayly, I.R. Gould, K.M. Merz, D.M. Ferguson, D.C. Spellmeyer, T. Fox, J.W. Caldwell, P.A. Kollman, A second generation force field for the simulation of proteins, nucleic acids, and organic molecules, J. Am. Chem. Soc, 117 (1995) 5179–5197.

[30] Darden, York, Pedersen, Particle mesh Ewald: An N·log(N) method for Ewald sums in large systems, J. Chem. Phys. 98 (1993) 10089–10092.

[31] K. Hinkle, C. Jameson, S. Murad, Transport of vanadium and oxovanadium ions across zeolite membranes: A molecular dynamics study, J. Phys. Chem. 118 (2014) 23803–23810.

[32] S. Plimpton, Fast parallel algorithms for short-range molecular dynamics, J. Comp. Phys. 117 (1995) 1–19, http://lammps.sandia.gov

[33] Z. Song, Y. Huang, W. L. Xu, L. Wang, Y. Bao, S. Li M. Yu, Continuously

adjustable, molecular-sieving “gate” on 5A zeolite for distinguishing small organic molecules by size, Scientific Reports. 5 (2015) 13981.

Table 1 PV results of NaA zeolite membranes for separation of 90 wt.% ethanol/water mixtures at 348K.

Membrane No.	J/kg m^{-2} h^{-1}	$\alpha_{water/ethanol}$
M1	1.58	8000
M2	1.91	15000

Table 2 Changes in zeolite cavity volume as a function of water loading

No. of water molecules in cavities	Contraction/expansion by %	Standard deviation
0	—	—
2	-0.030014391	0.00285841
4	-0.020720174	0.002324976
6	-0.017396228	0.003512176
8	-0.009837187	0.002150134
16	0.008778982	0.002502852
20	0.014984884	0.002763588
39	0.07909061	0.002727784

Figure captions

Fig. 1 Schematic diagram of VP dehydration apparatus for NaA zeolite membrane.

Fig. 2 Schematic of the simulation system for VP through NaA zeolite membrane.

Fig. 3 Surface and cross-section SEM images of NaA zeolite membranes M1 (a, b) and M2 (c, d).

Fig. 4 VP separation results of M1 for binary water/alcohol (methanol, ethanol and IPA) mixtures at 373 K as a function of feed water content: (a) water and alcohol fluxes, (b) separation factor.

Fig. 5 VP separation results of M2 for binary water/alcohol (methanol, ethanol and IPA) mixtures at 373 K as a function of feed water content: (a) water and alcohol fluxes; (b) separation factor.

Fig. 6 Permeation number of IPA molecules as a function of time under different feed water contents.

Fig. 7 Contrasting behavior with pure IPA (left side, a, c, and e) and with 5 wt.% water (right side, b, d and f): (a) axial view of the defect showing pure IPA molecules permeating the defect; (b) axial view of the defect showing water and IPA molecules blocking the defect; (c) as (a) above but with IPA molecules not shown; (d) as (b) above but IPA molecules not shown; (e) cross section view showing pure IPA in cavity; (f) cross section view showing both water and IPA molecules in cavity. The spheres represent: green,

zeolite framework sites; yellow, defect sites; orange, IPA sites; blue, water. The spheres to ease viewing are not to scale.

Fig. 8 Change in phase behavior of vapor phase when water is present: (a) snapshot of the pure IPA vapor phase (away from membrane); (b) snapshot with 5 wt.% water in vapor phase (away from membrane).

Fig. 9 Helium flux of NaA zeolite membrane at 313 K as a function of (a) water activity under pressure drop of 20 kPa and 100 kPa; and (b) alcohol (methanol, ethanol and IPA) activity under pressure drop of 100 kPa.

Fig. 10 VP separation results of M1 for water/IPA, water/IPA/6 wt.% methanol and water/IPA/6 wt.% ethanol mixtures at 373 K as a function of feed water content: (a) water flux and water/IPA selectivity; (b) IPA flux.

Fig. 11 VP separation results of M1 for 3 wt.% water/IPA/methanol and 3 wt.% water/IPA/ethanol mixtures at 373 K as a function of feed methanol or ethanol content: (a) water flux and IPA flux; (b) water/IPA selectivity.

Fig. 12 VP separation results of NaA zeolite membrane for water/*n*-butanol, water/*n*-butanol/19 wt.% methanol and water/*n*-butanol/19 wt.% ethanol mixtures at 393 K as a function of feed water content: (a) water flux and water/*n*-butanol selectivity; (b) *n*-

butanol flux.

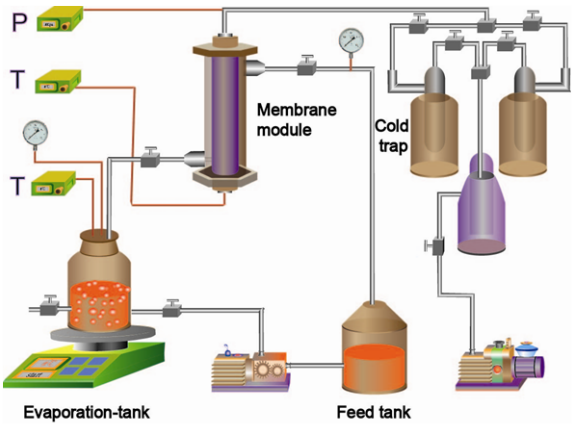

Fig. 1 Schematic diagram of VP dehydration apparatus for NaA zeolite membrane.

Fig. 2 Schematic of the simulation system for VP through NaA zeolite membrane.

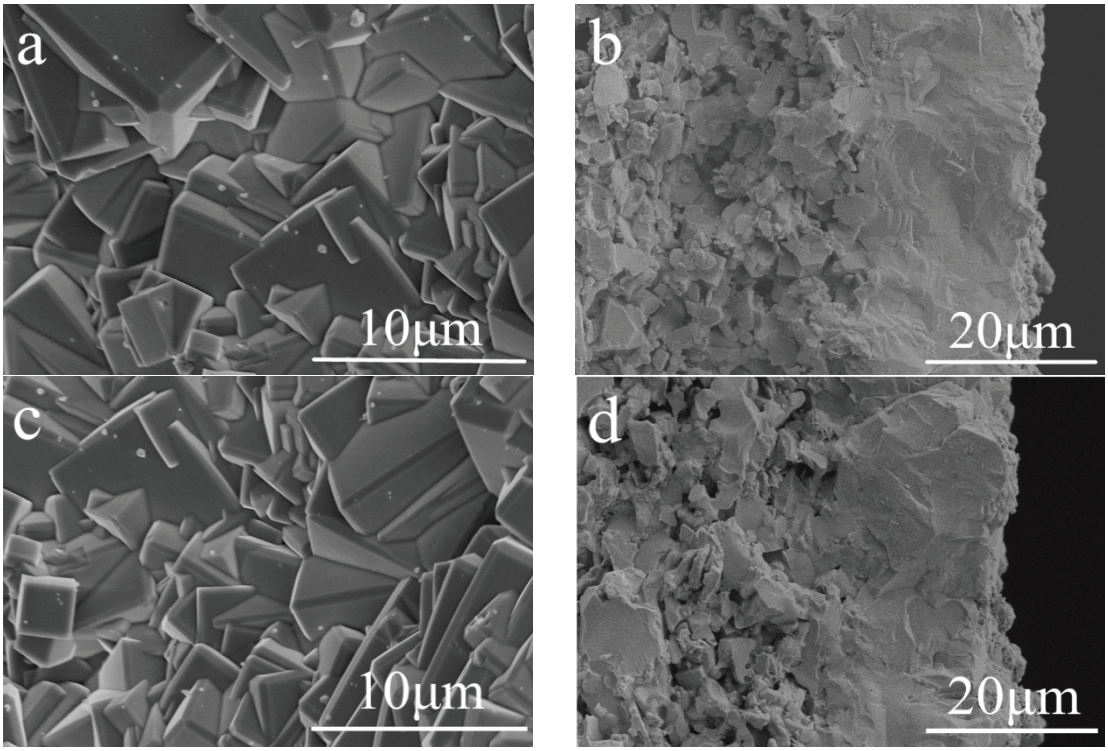

Fig. 3 Surface and cross-section SEM images of NaA zeolite membranes M1 (a, b) and M2 (c, d).

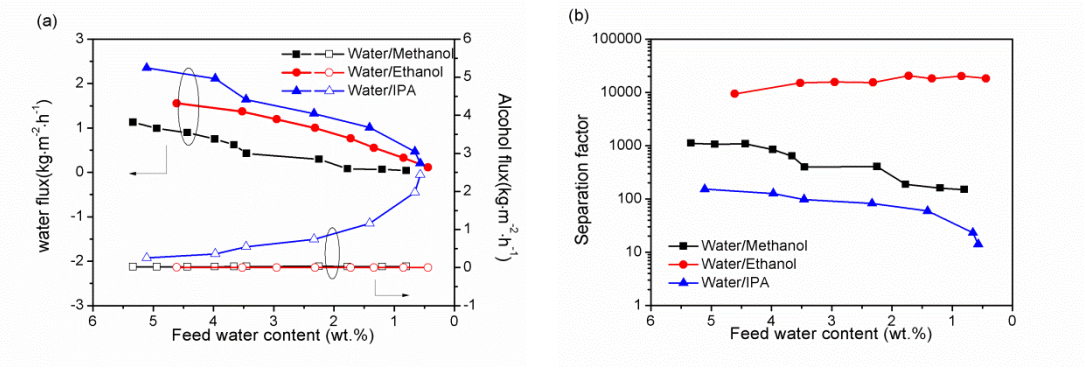

Fig.4 VP separation results of M1 for binary water/alcohol (methanol, ethanol and IPA) mixtures at 373 K as a function of feed water content: (a) water and alcohol fluxes, (b) separation factor.

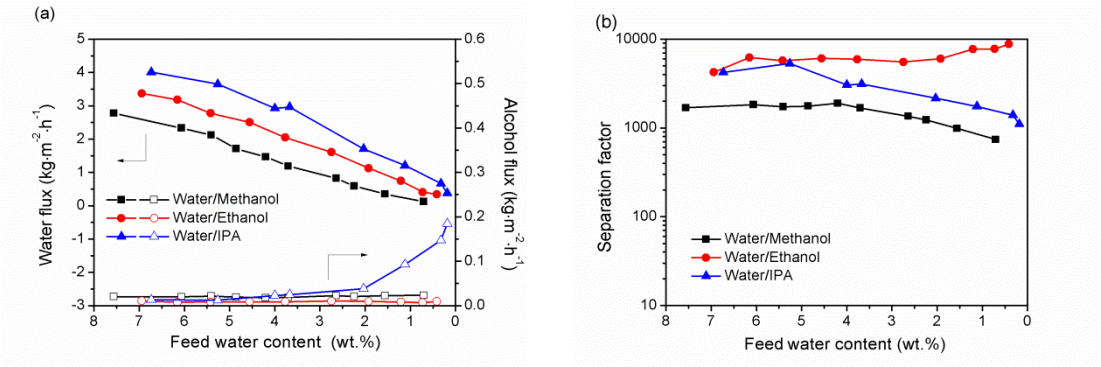

Fig. 5 VP separation results of M2 for binary water/alcohol (methanol, ethanol and IPA) mixtures at 373 K as a function of feed water content: (a) water and alcohol fluxes; (b) separation factor.

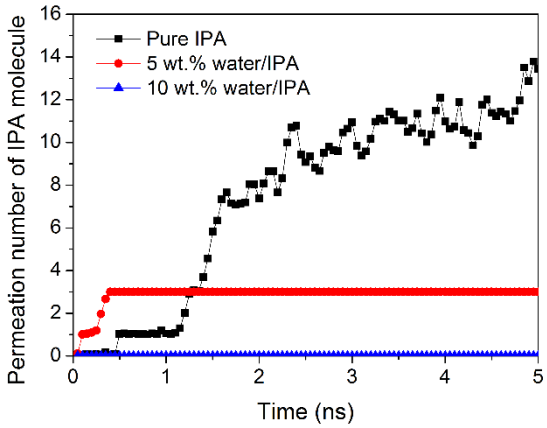

Fig. 6 Permeation number of IPA molecule as a function of time under different feed water contents.

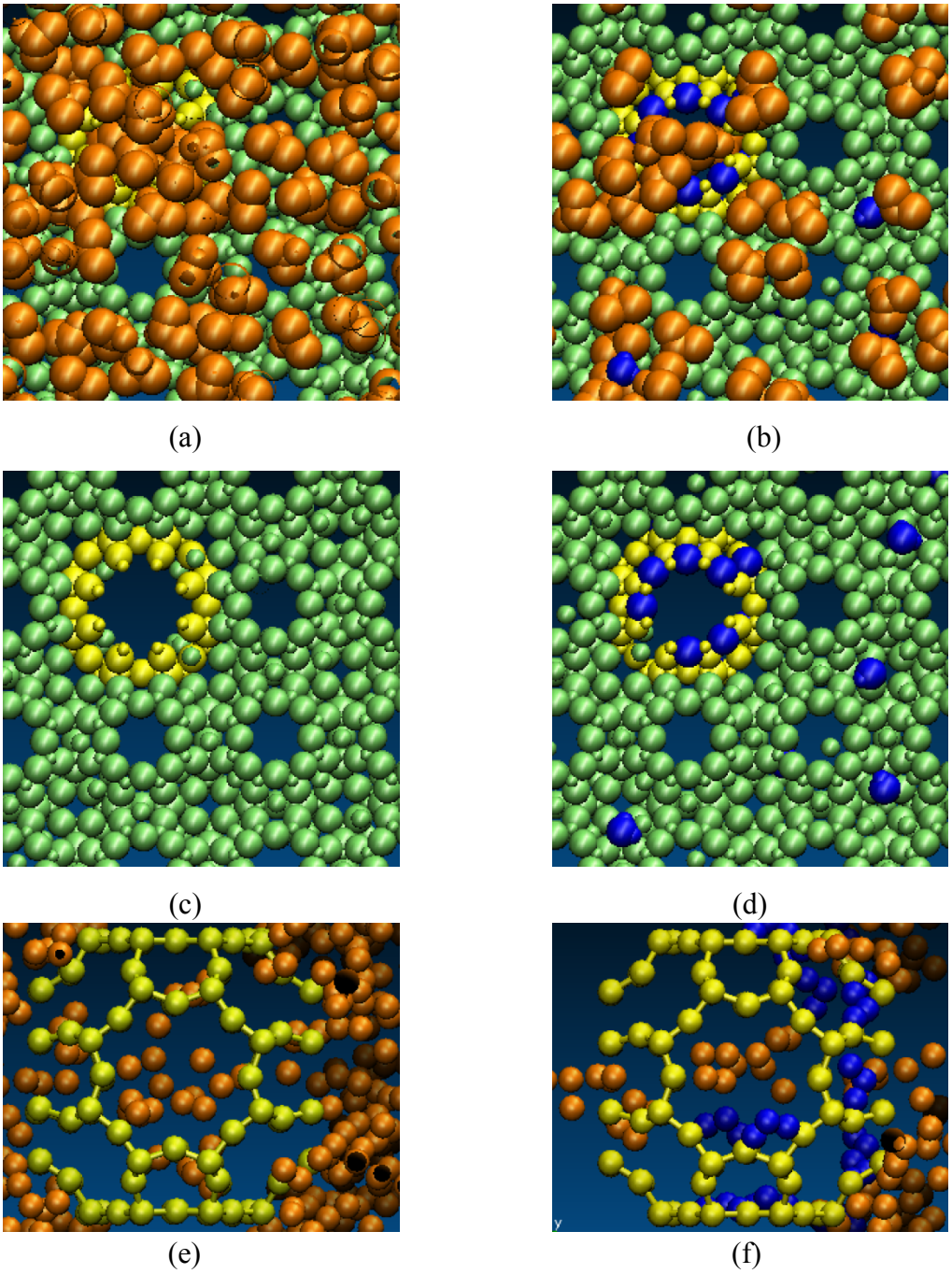

Fig. 7 Contrasting behavior with pure IPA (left side, a, c, and e) and with 5 wt.% water (right side, b, d and f): (a) axial view of the defect showing pure IPA molecules permeating the defect; (b) axial view of the defect showing water and IPA molecules blocking the defect; (c) as (a) above but with IPA molecules not shown; (d) as (b) above but IPA molecules not shown; (e) cross section view showing pure IPA in cavity; (f) cross section view showing both water and IPA molecules in cavity. The

spheres represent: green, zeolite framework sites; yellow, defect sites; orange, IPA sites; blue, water. The spheres to ease viewing are not to scale.

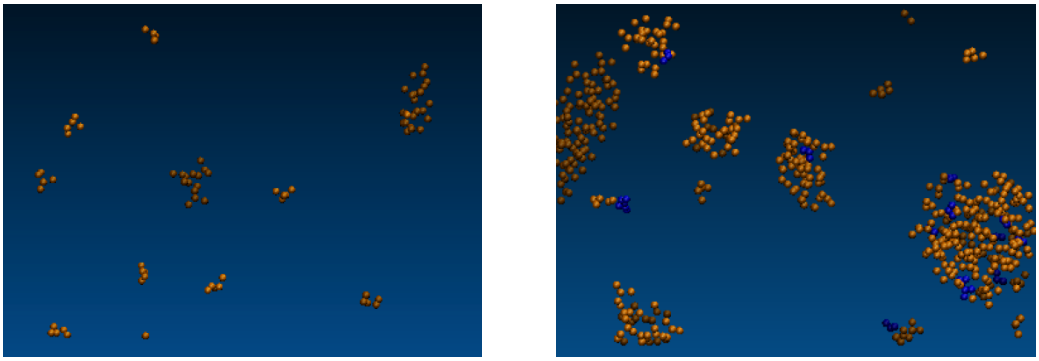

(a) (b)

Fig. 8 Change in phase behavior of vapor phase when water is present: (a) snapshot of the pure IPA vapor phase (away from membrane); (b) snapshot with 5 wt.% water in vapor phase (away from membrane).

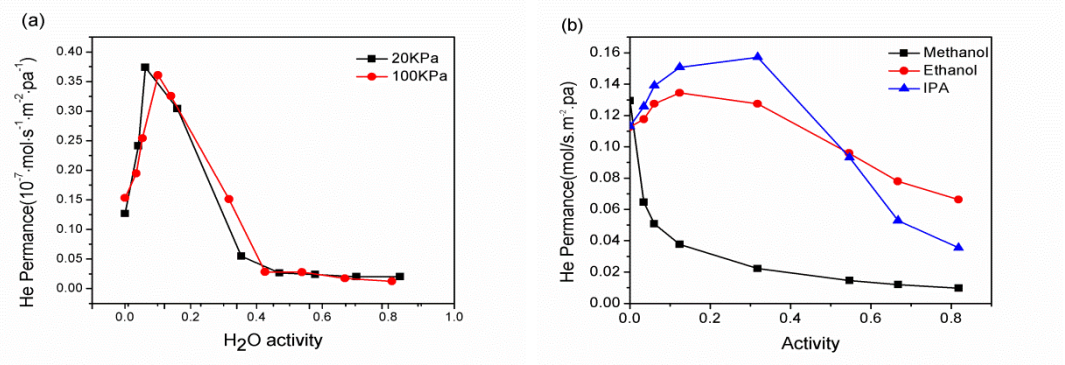

Fig. 9 Helium flux of NaA zeolite membrane at 313 K as a function of (a) water activity under pressure drop of 20 kPa and 100 kPa; and (b) alcohol (methanol, ethanol and IPA) activity under pressure drop of 100 kPa.

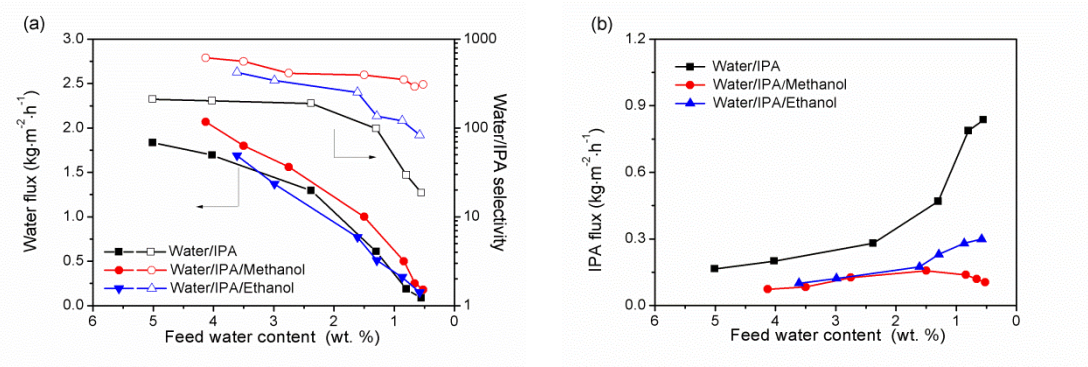

Fig. 10 VP separation results of M1 for water/IPA, water/IPA/6 wt.% methanol and water/IPA/6 wt.% ethanol mixtures at 373 K as a function of feed water content: (a) water flux and water/IPA selectivity; (b) IPA flux.

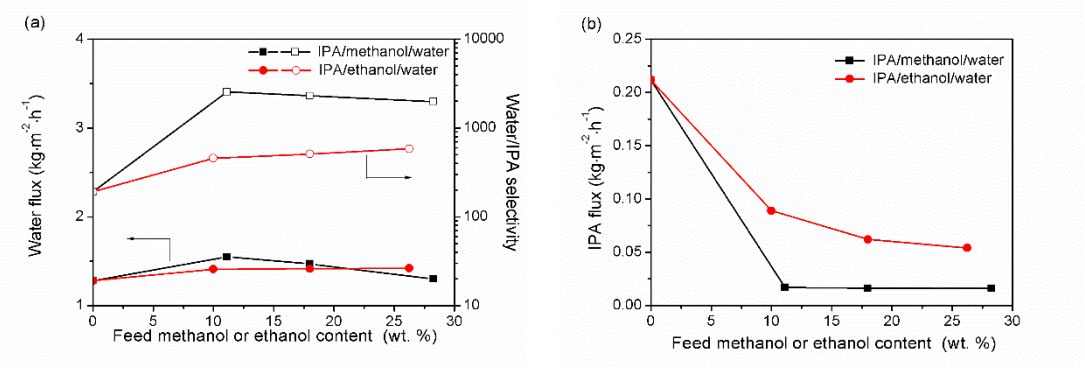

Fig. 11 VP separation results of M1 for 3 wt.% water/IPA/methanol and 3 wt.% water/IPA/ethanol mixtures at 373 K as a function of feed methanol or ethanol content: (a) water flux and water/IPA selectivity; (b) IPA flux.

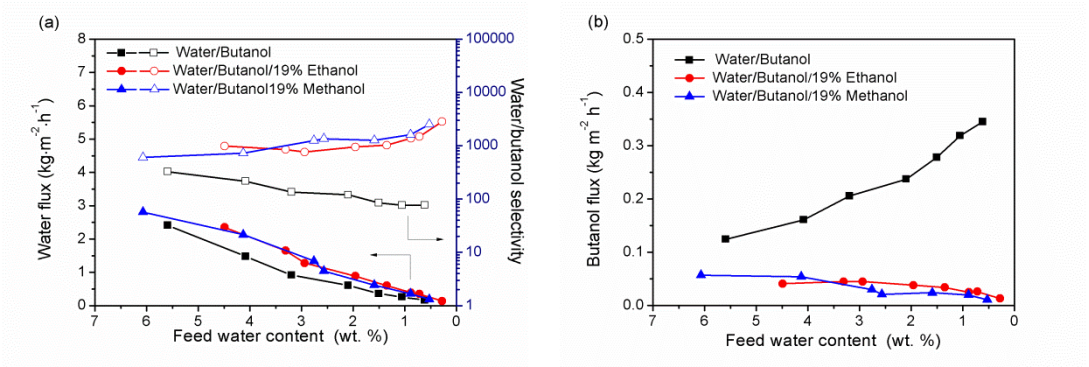

Fig. 12 VP separation results of NaA zeolite membrane for water/*n*-butanol, water/*n*-butanol/19 wt.% methanol and water/*n*-butanol/19 wt.% ethanol mixtures at 393 K as a function of feed water content: (a) water flux and water/*n*-butanol selectivity; (b) *n*-butanol flux.

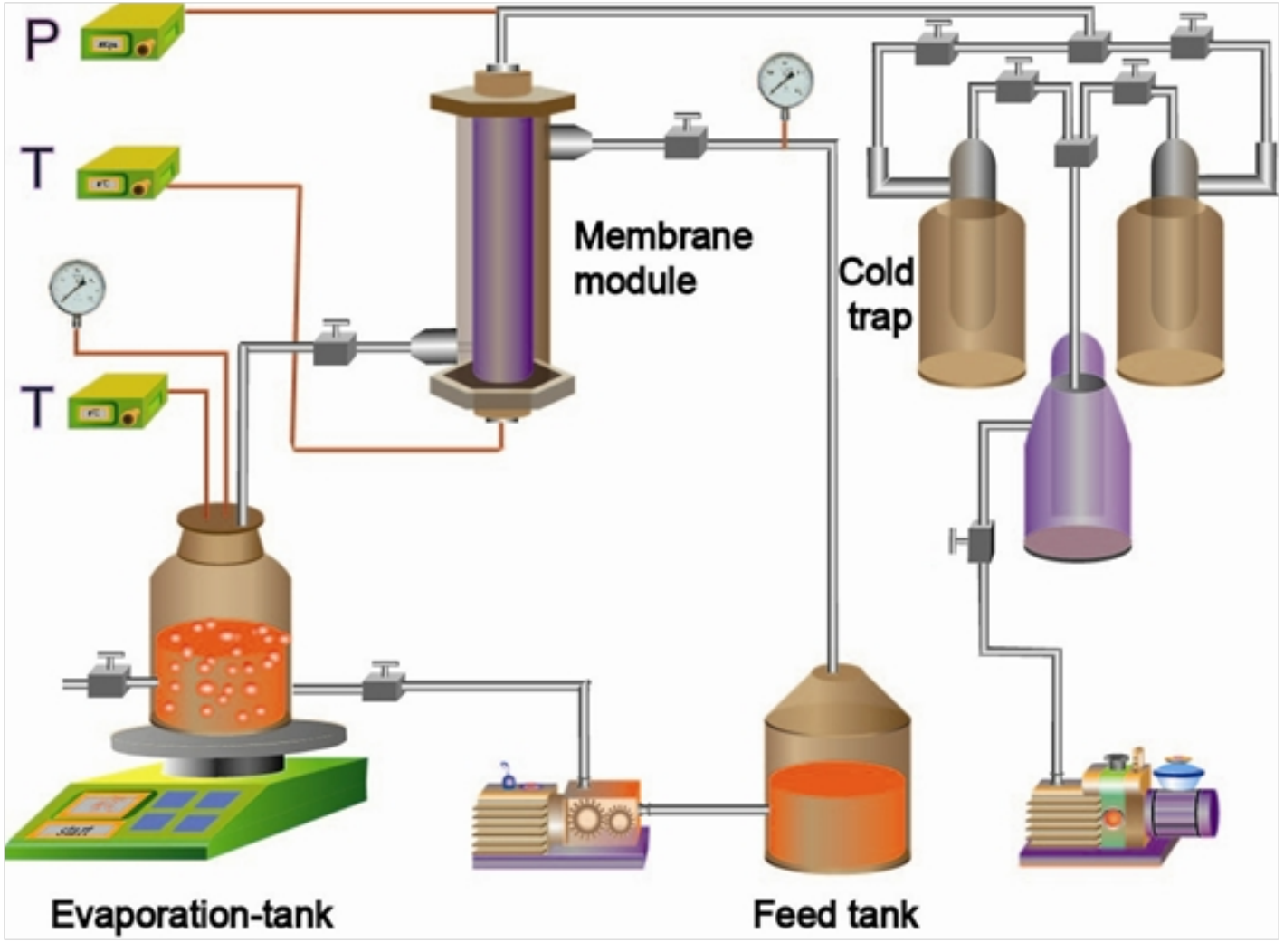
P
T
T
Membrane module
Cold trap
Evaporation-tank
Feed tank

membrane

Vapor Phase

membrane

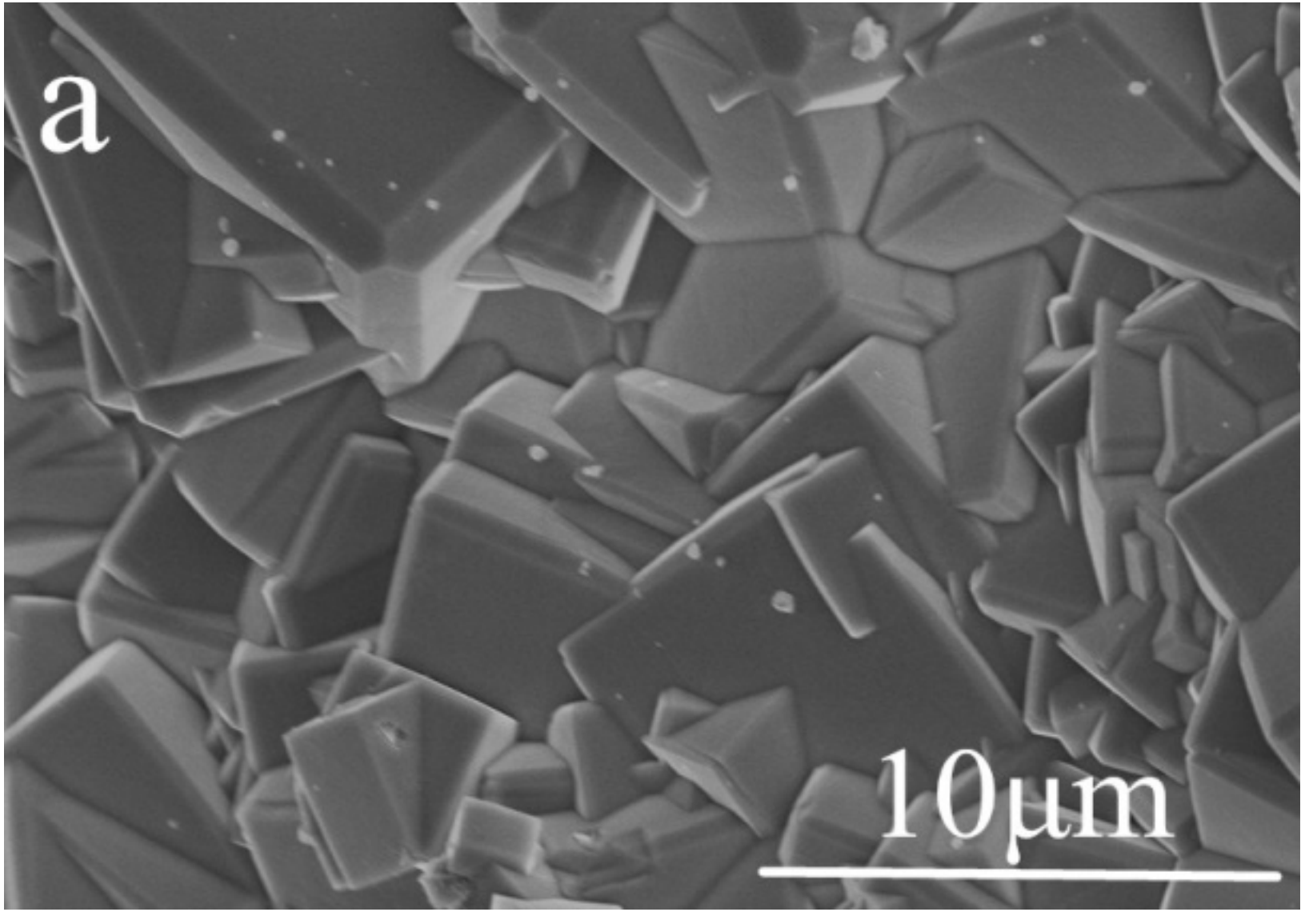
a
10μm

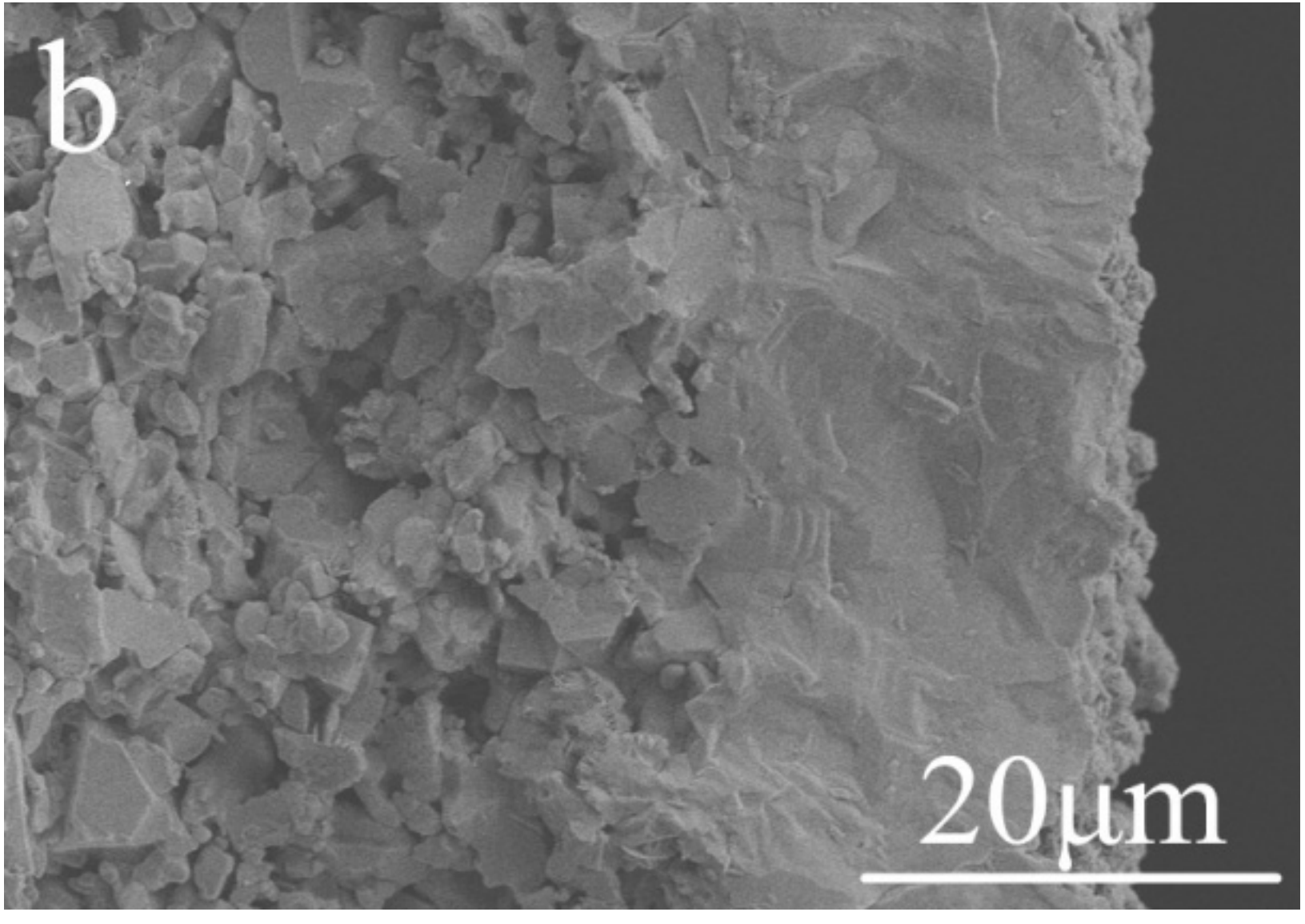
b
20μm

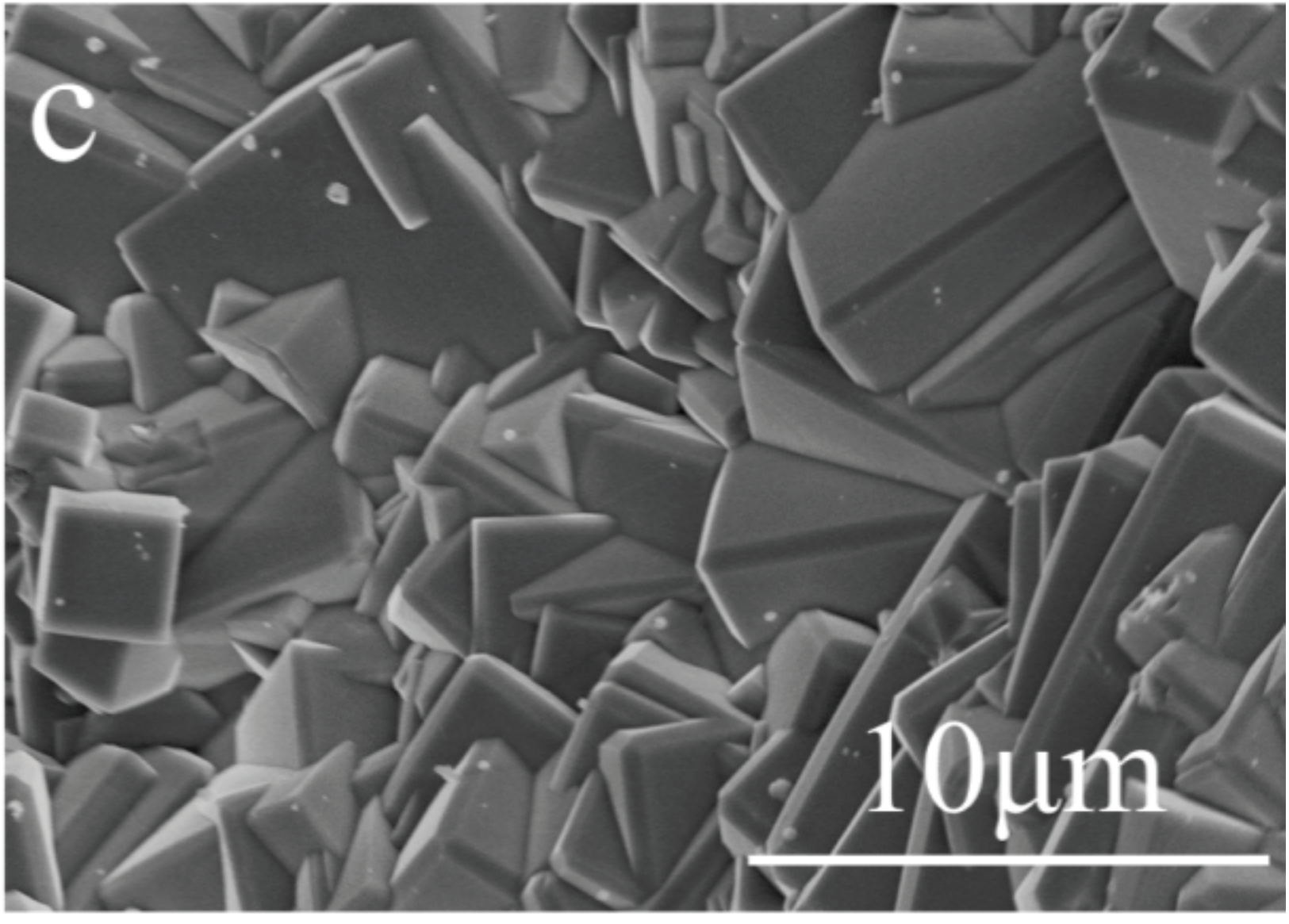
c
10μm

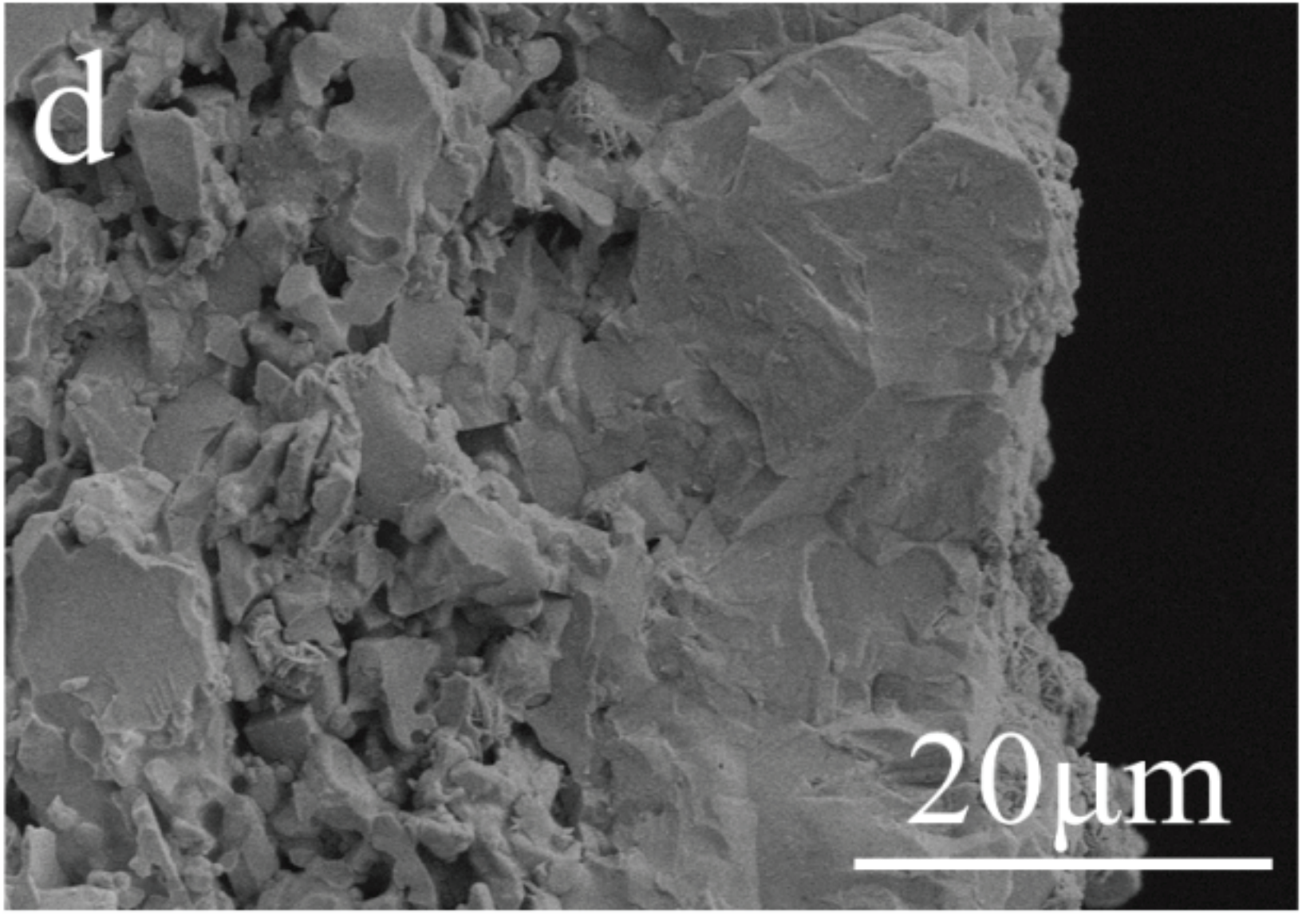
d
20μm

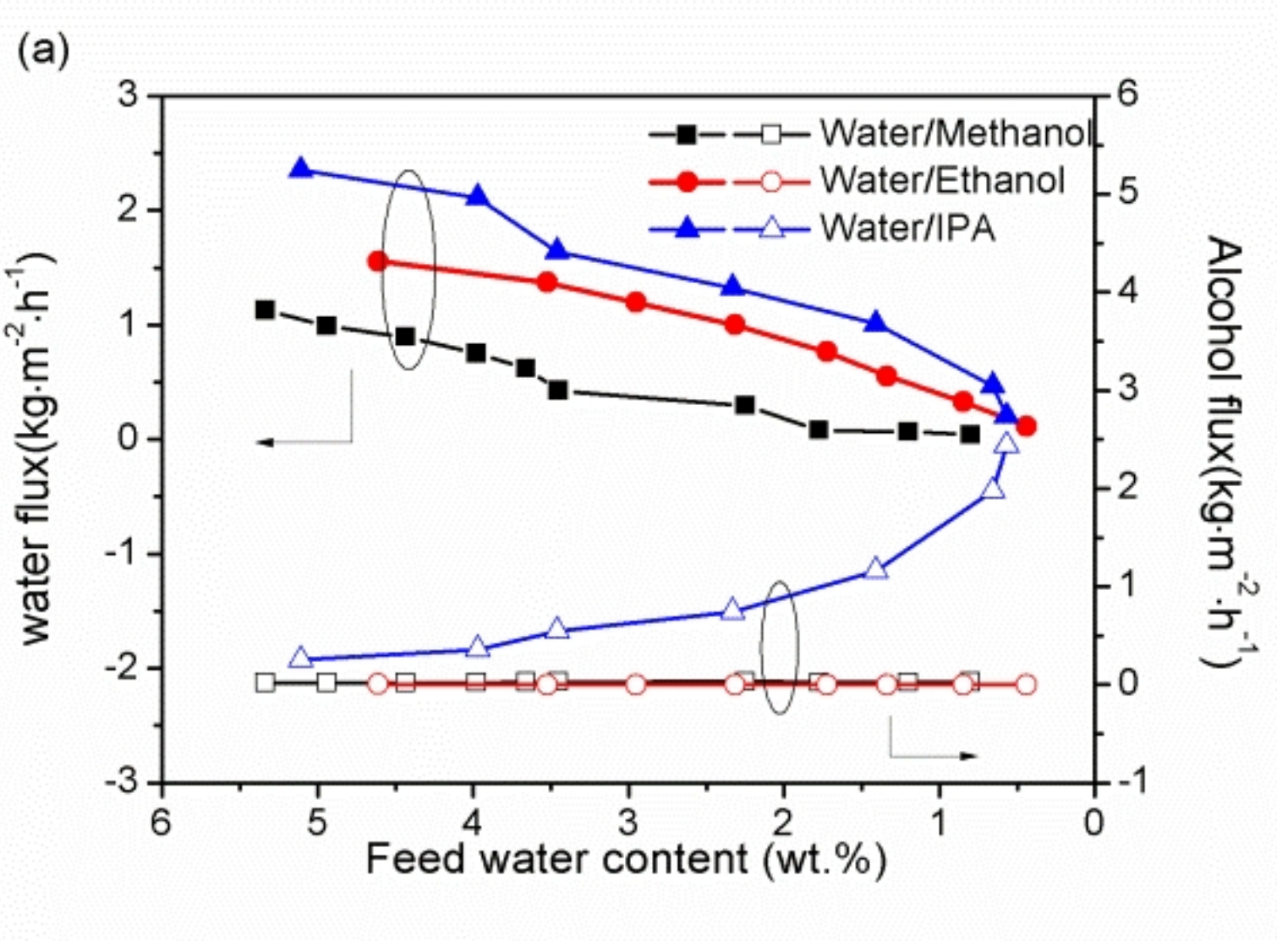
(a)
Water/Methanol
Water/Ethanol
Water/IPA
water flux(kg·m-2·h-1)
Alcohol flux(kg·m-2·h-1)
Feed water content (wt.%)
3
2
1
0
-1
-2
-3
6
5
4
3
2
1
0
-1

(b)

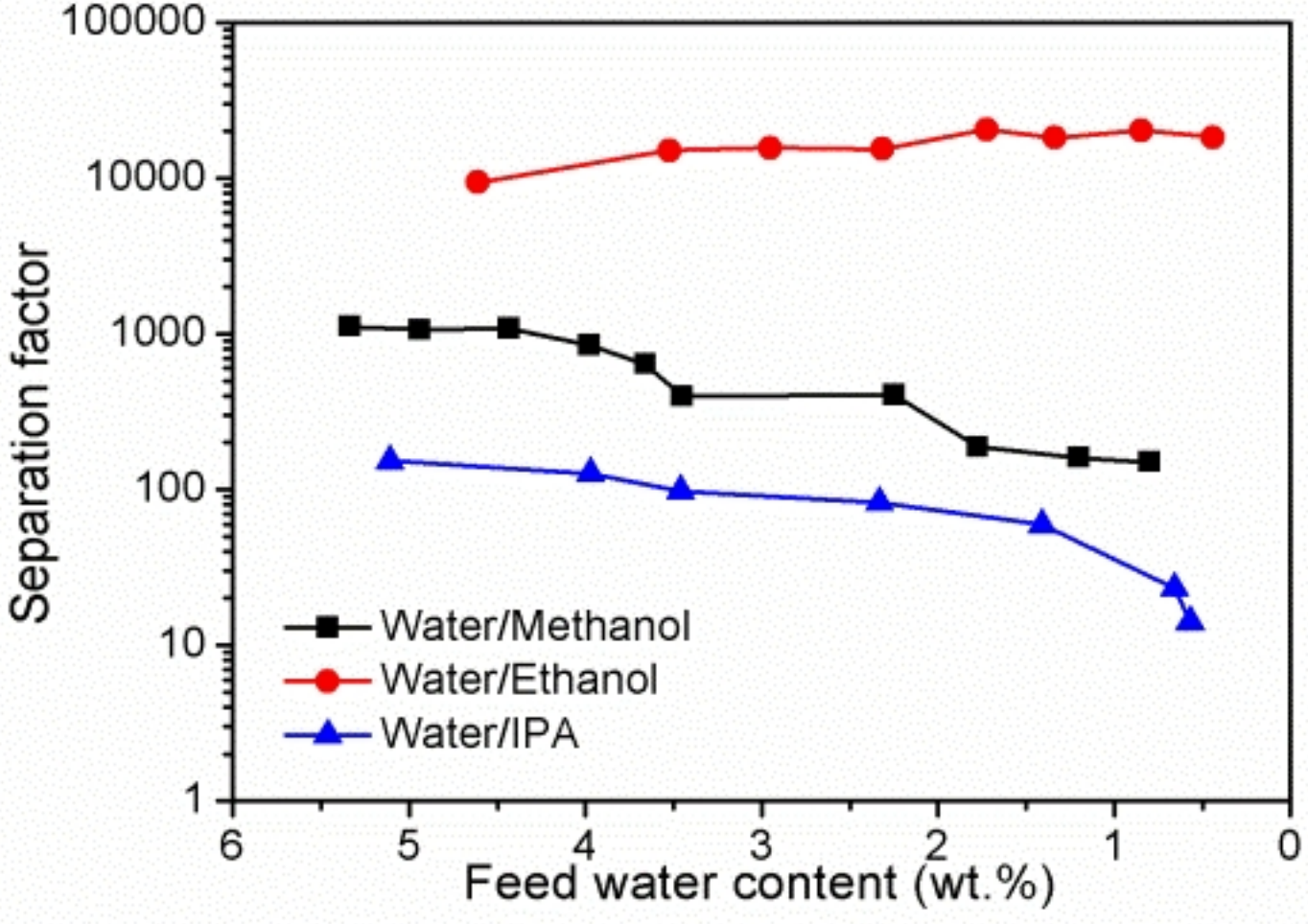
100000
10000
1000
100
10
1
Separation factor
6
5
4
3
2
1
0
Feed water content (wt.%)
Water/Methanol
Water/Ethanol
Water/IPA

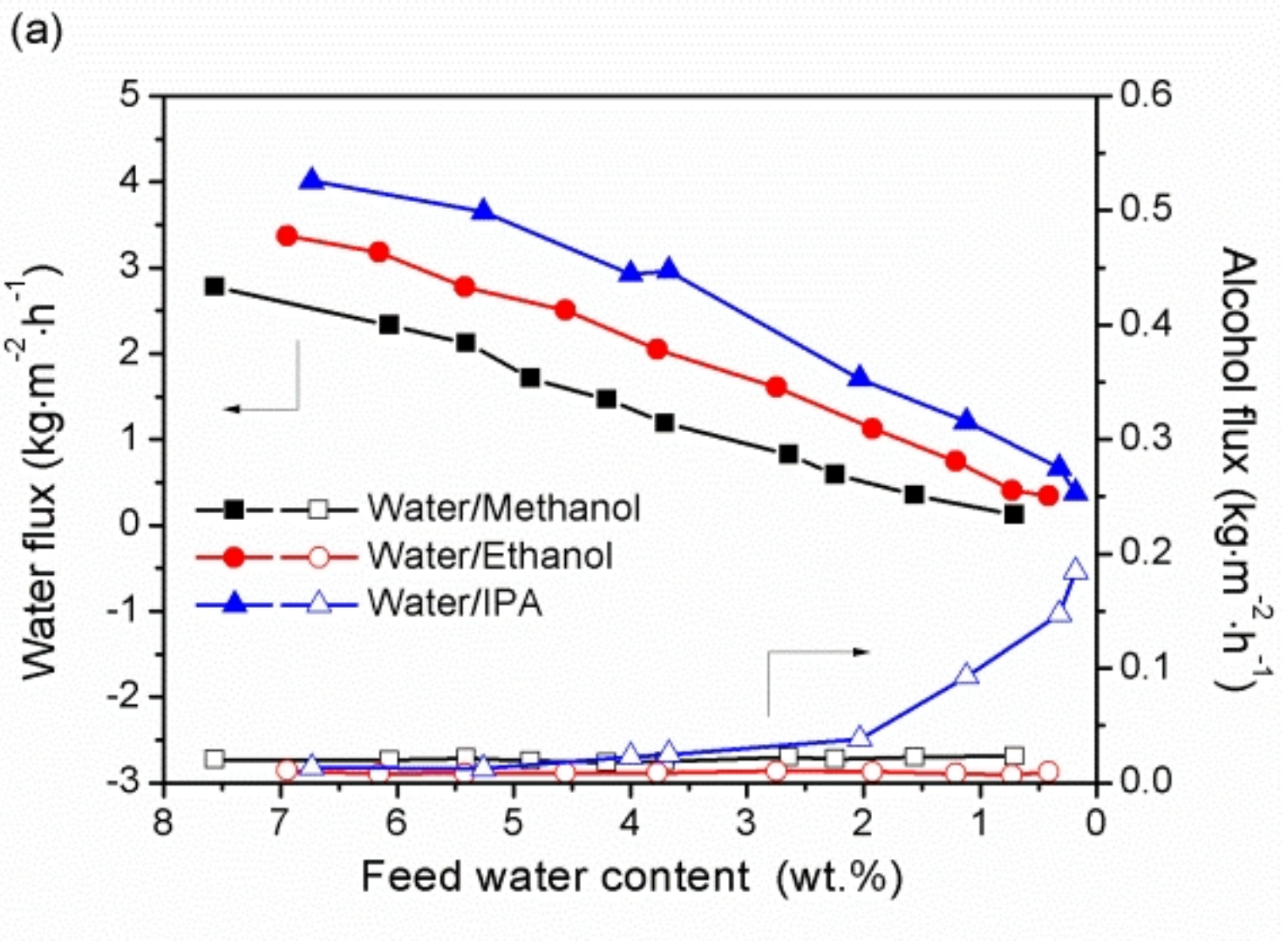
(a)
Water flux (kg·m-2·h-1)
Alcohol flux (kg·m-2·h-1)
Feed water content (wt.%)
Water/Methanol
Water/Ethanol
Water/IPA
5
4
3
2
1
0
-1
-2
-3
0.6
0.5
0.4
0.3
0.2
0.1
0.0
8
7
6
5
4
3
2
1
0

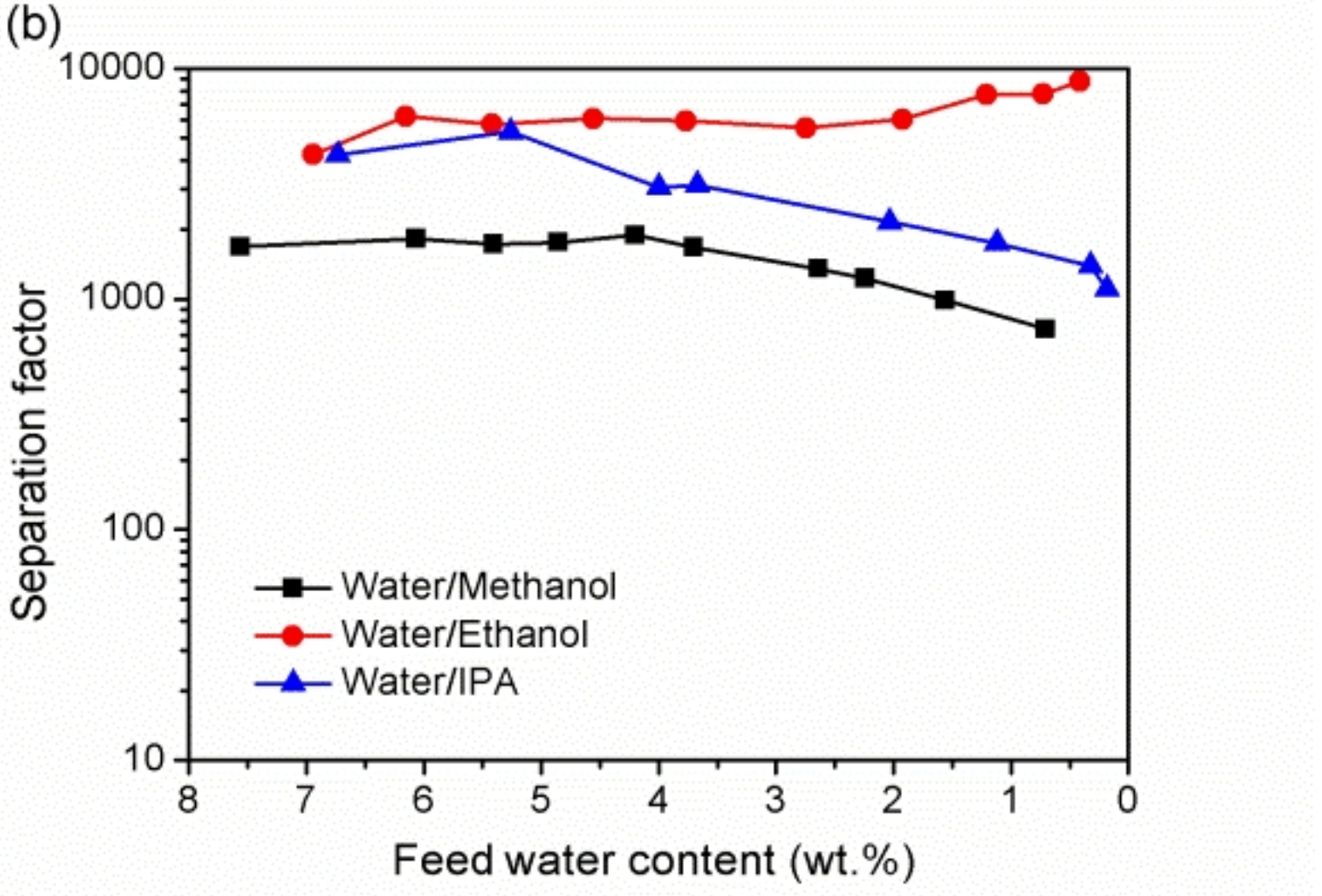
(b)
10000
1000
100
10
Separation factor
Water/Methanol
Water/Ethanol
Water/IPA
8
7
6
5
4
3
2
1
0
Feed water content (wt.%)

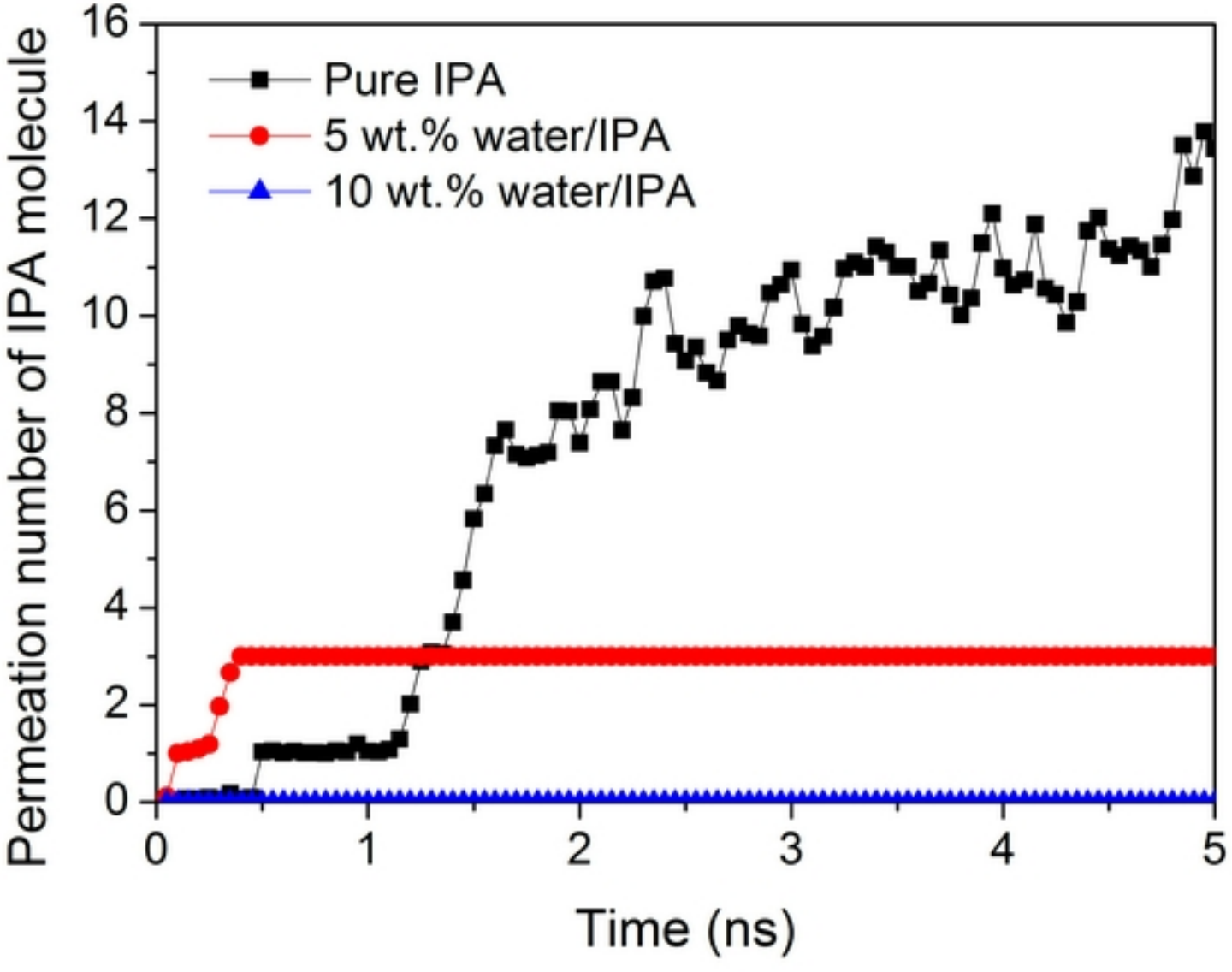
Pure IPA
5 wt.% water/IPA
10 wt.% water/IPA
Permeation number of IPA molecule
Time (ns)
0
2
4
6
8
10
12
14
16
0
1
2
3
4
5

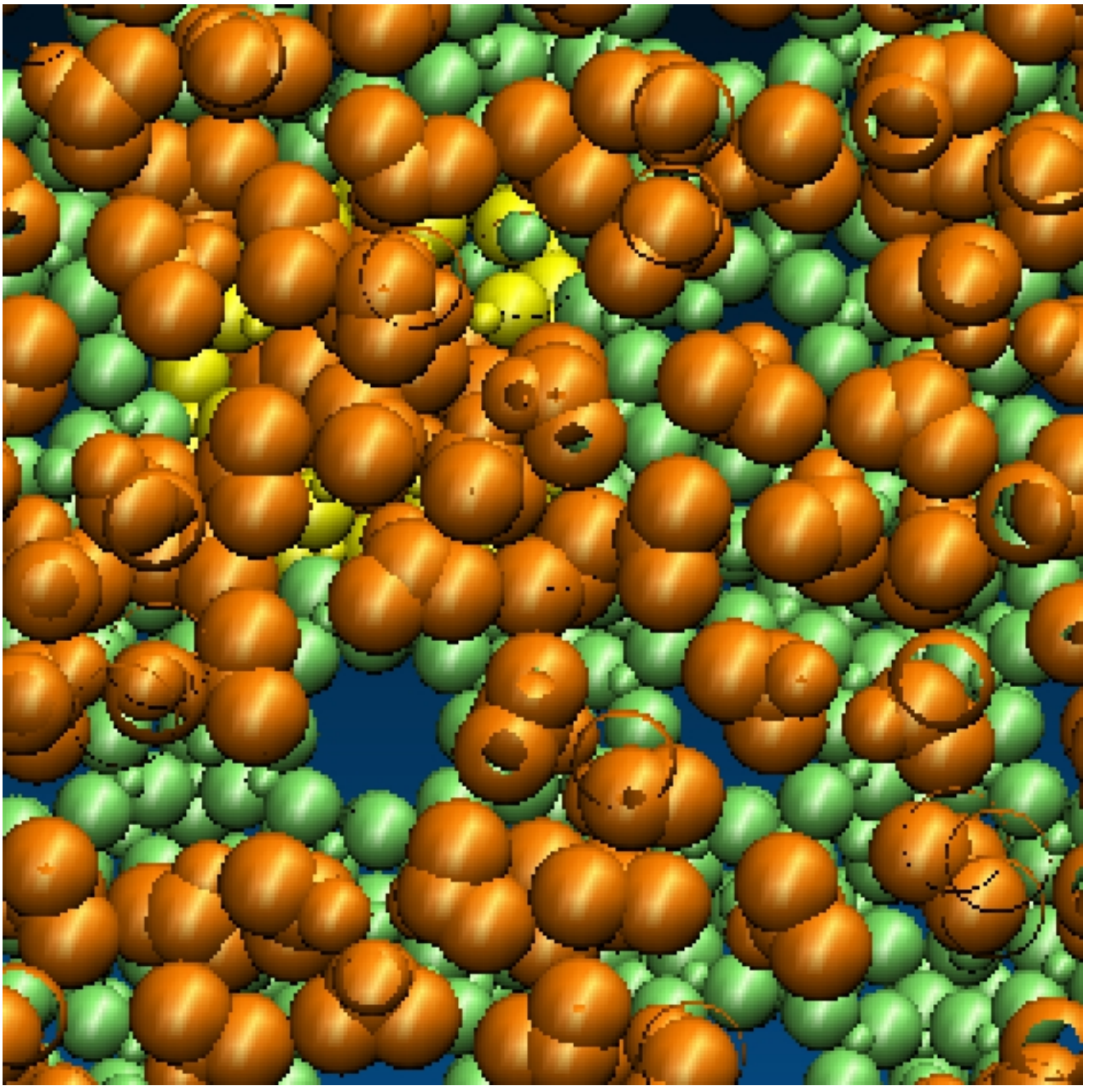

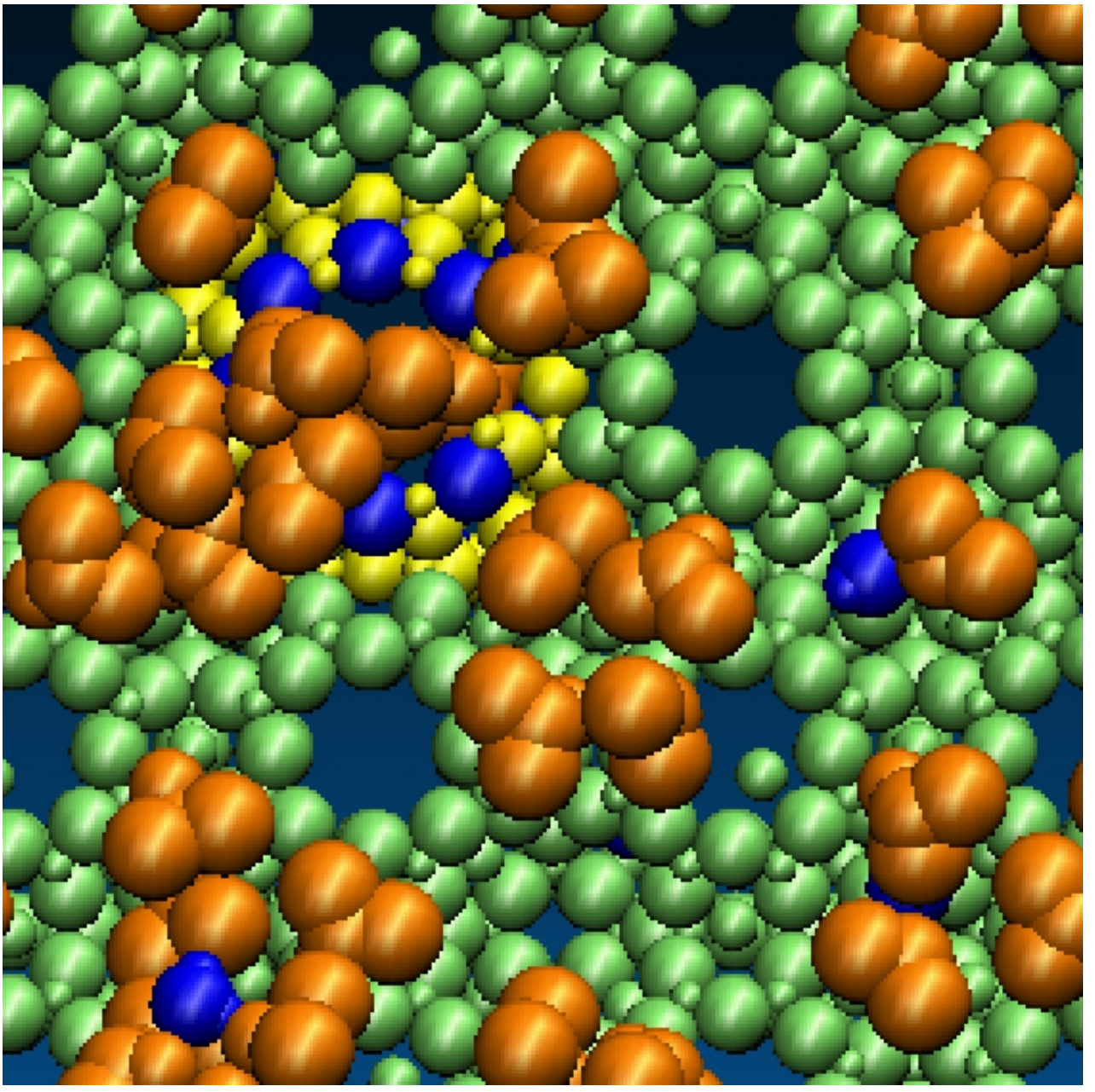

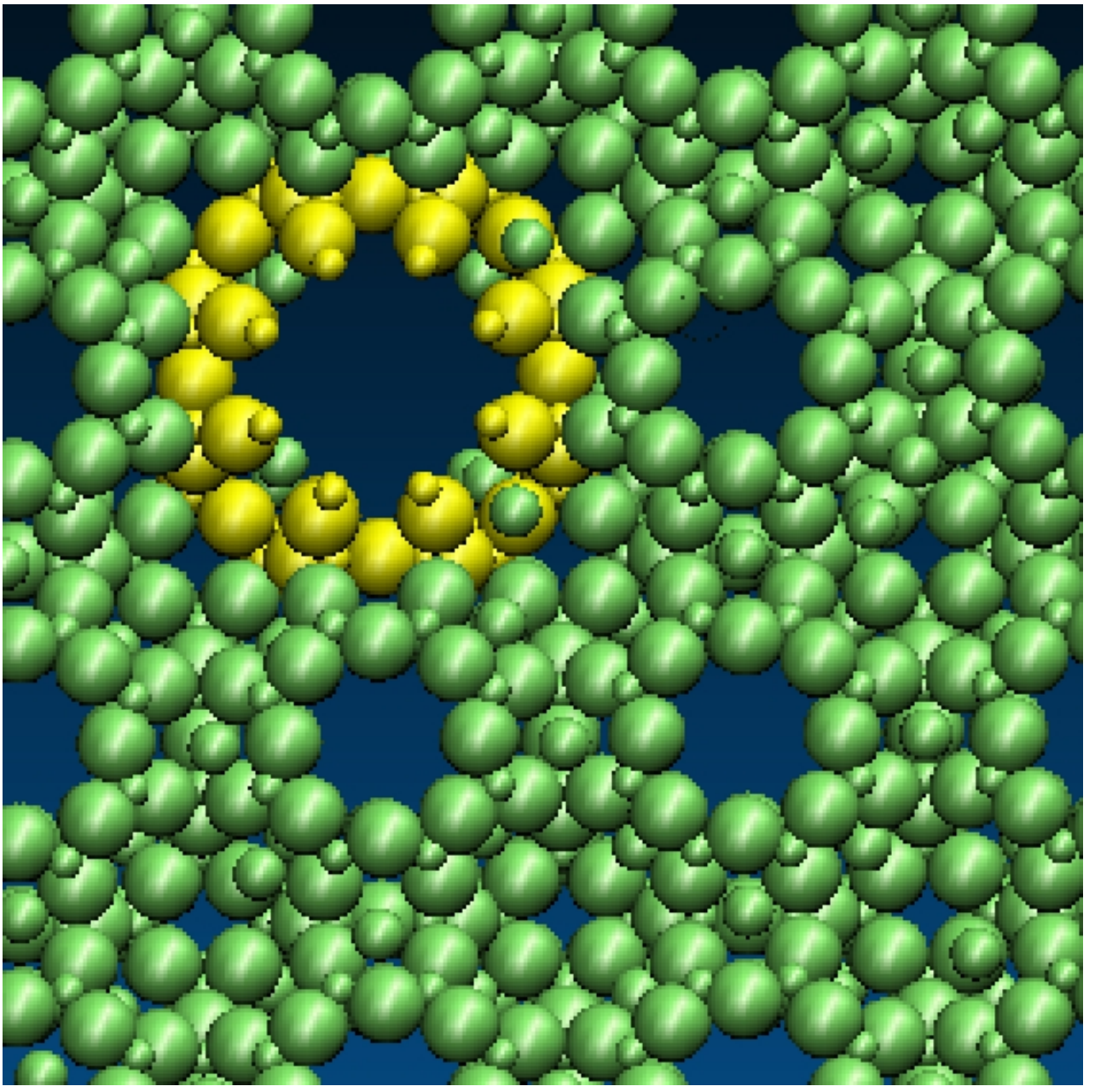

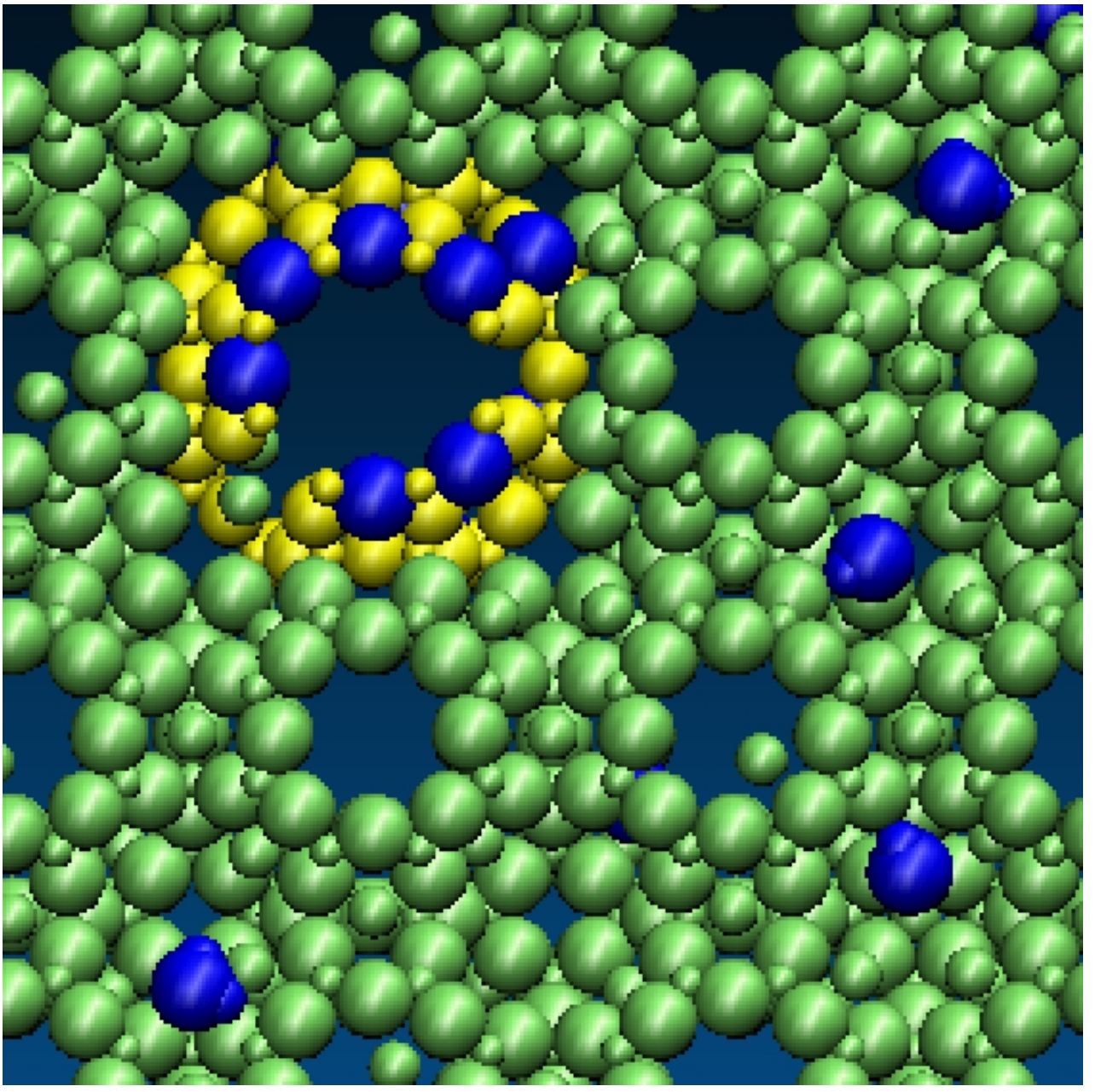

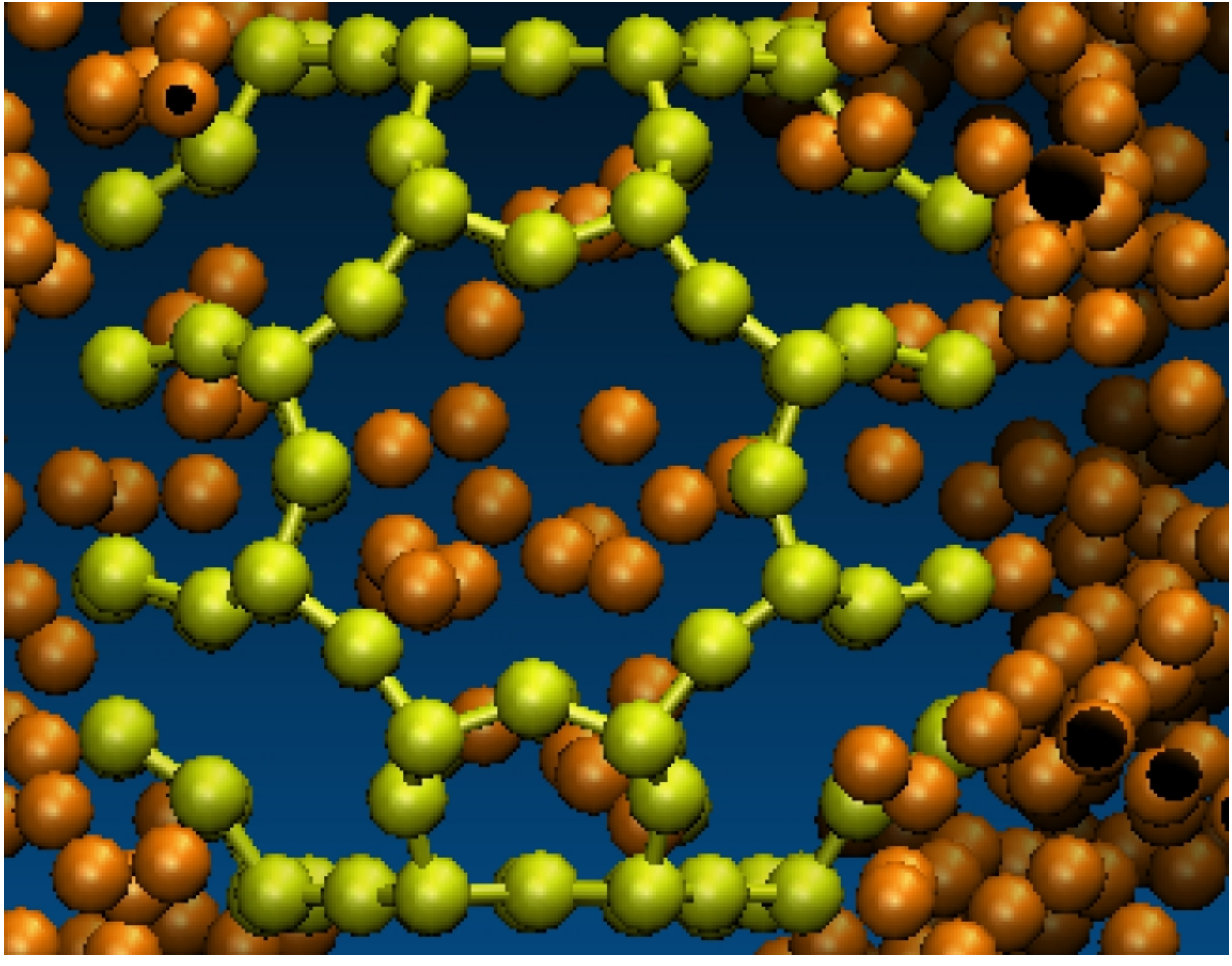

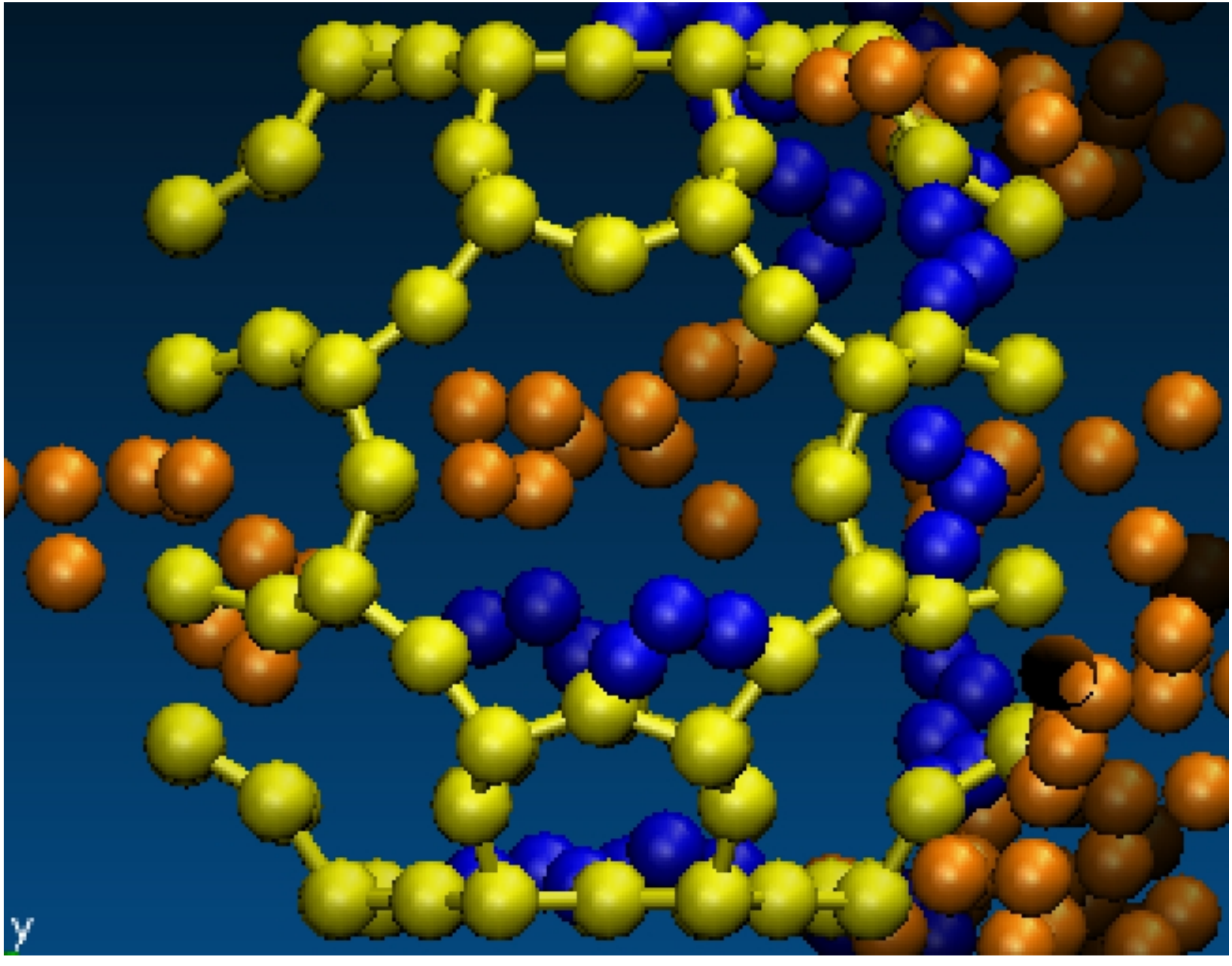
y

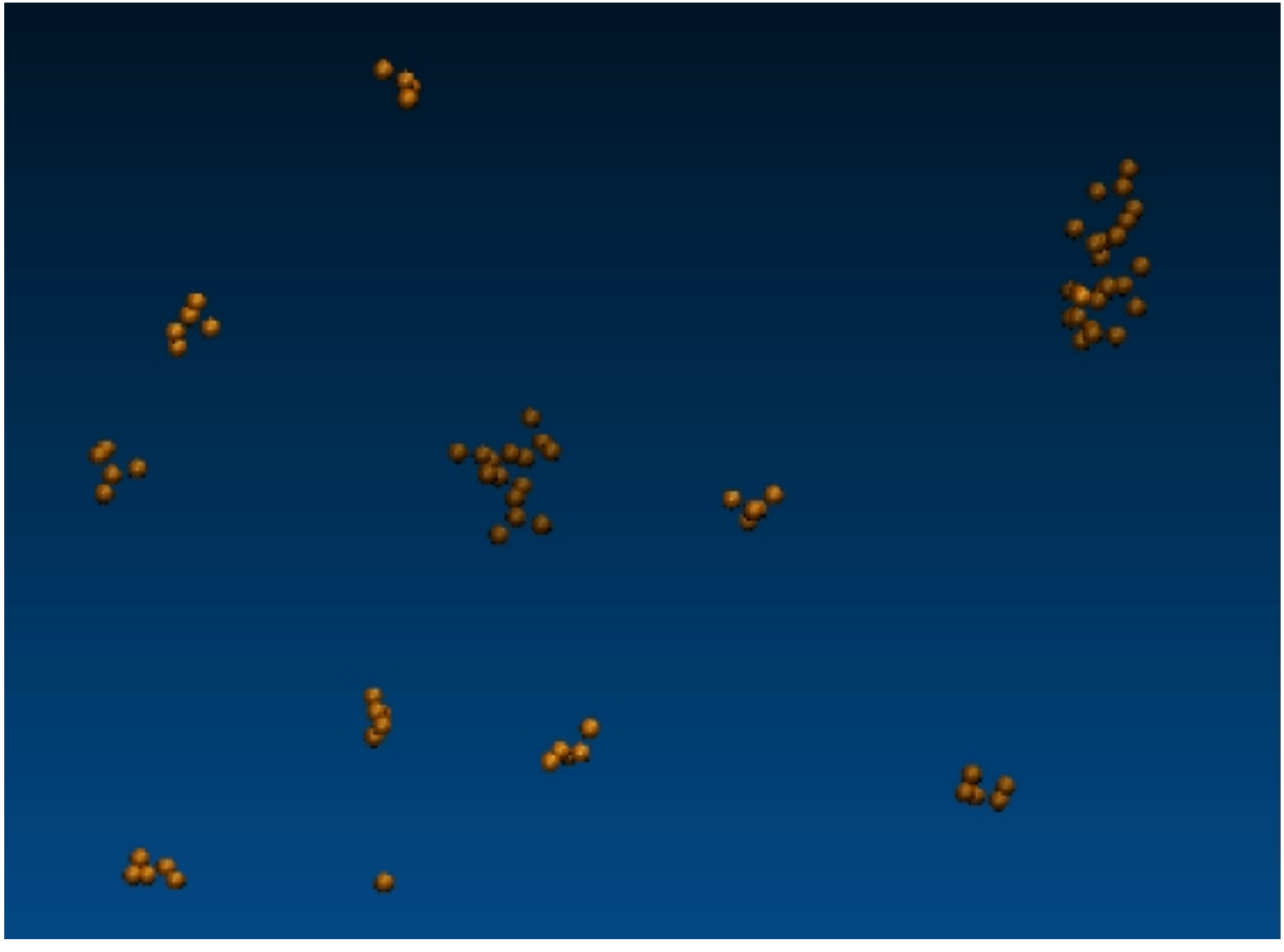

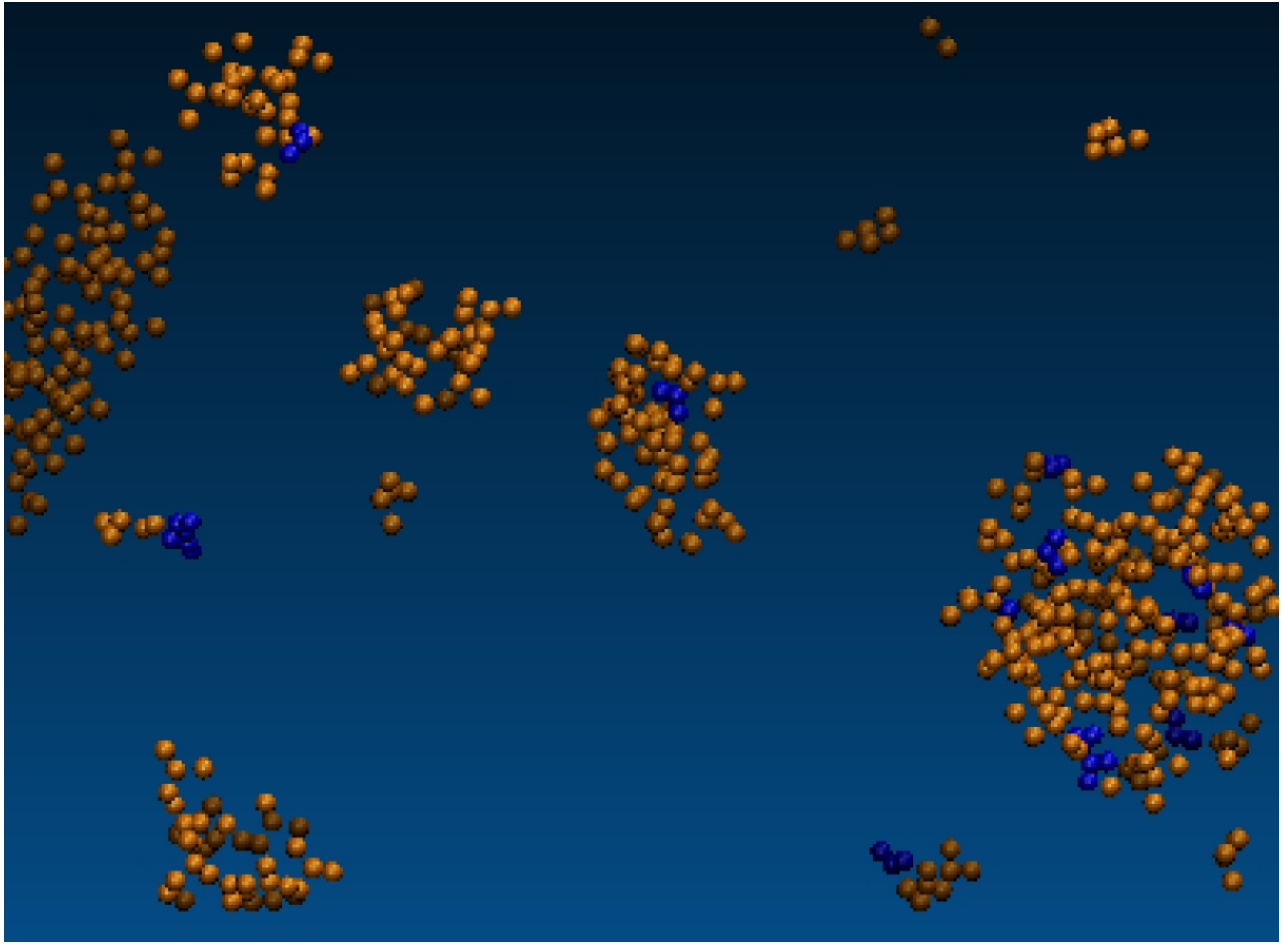

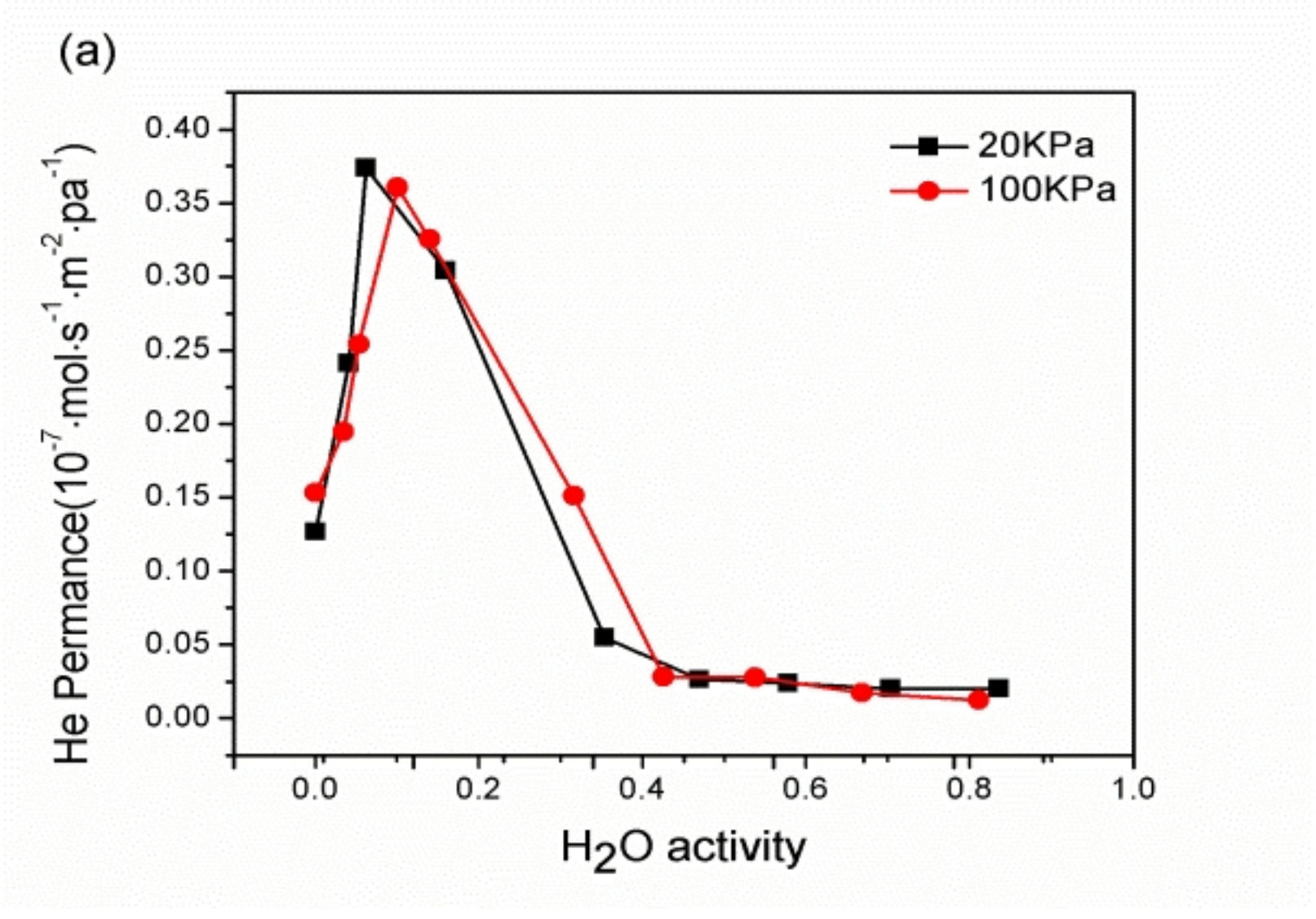
(a)
He Permance(10^{-7}·mol·s^{-1}·m^{-2}·pa^{-1})
0.40
0.35
0.30
0.25
0.20
0.15
0.10
0.05
0.00
0.0
0.2
0.4
0.6
0.8
1.0
H_2O activity
20KPa
100KPa

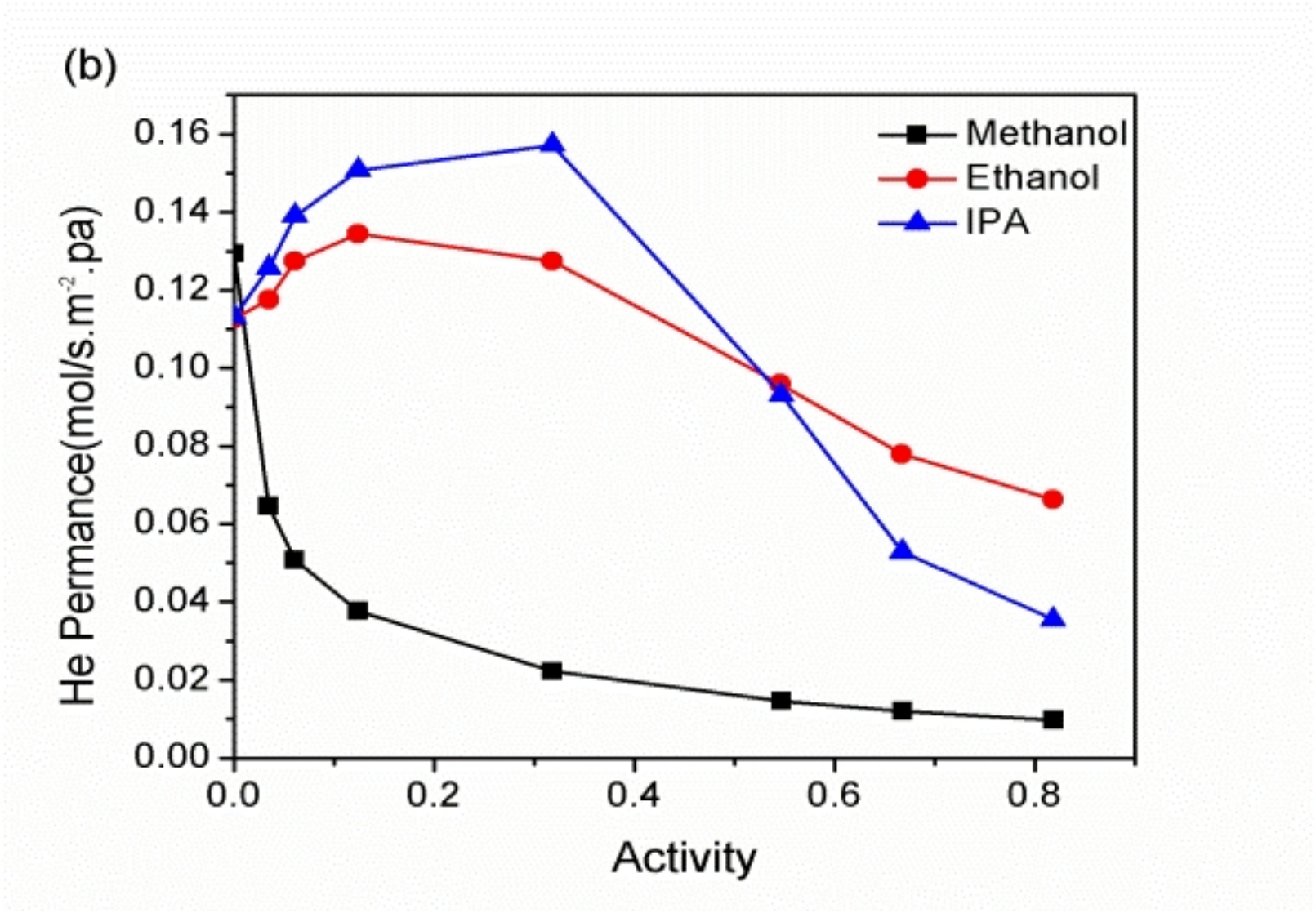
(b)
He Permance(mol/s.m-2.pa)
0.16
0.14
0.12
0.10
0.08
0.06
0.04
0.02
0.00
0.0
0.2
0.4
0.6
0.8
Activity
Methanol
Ethanol
IPA

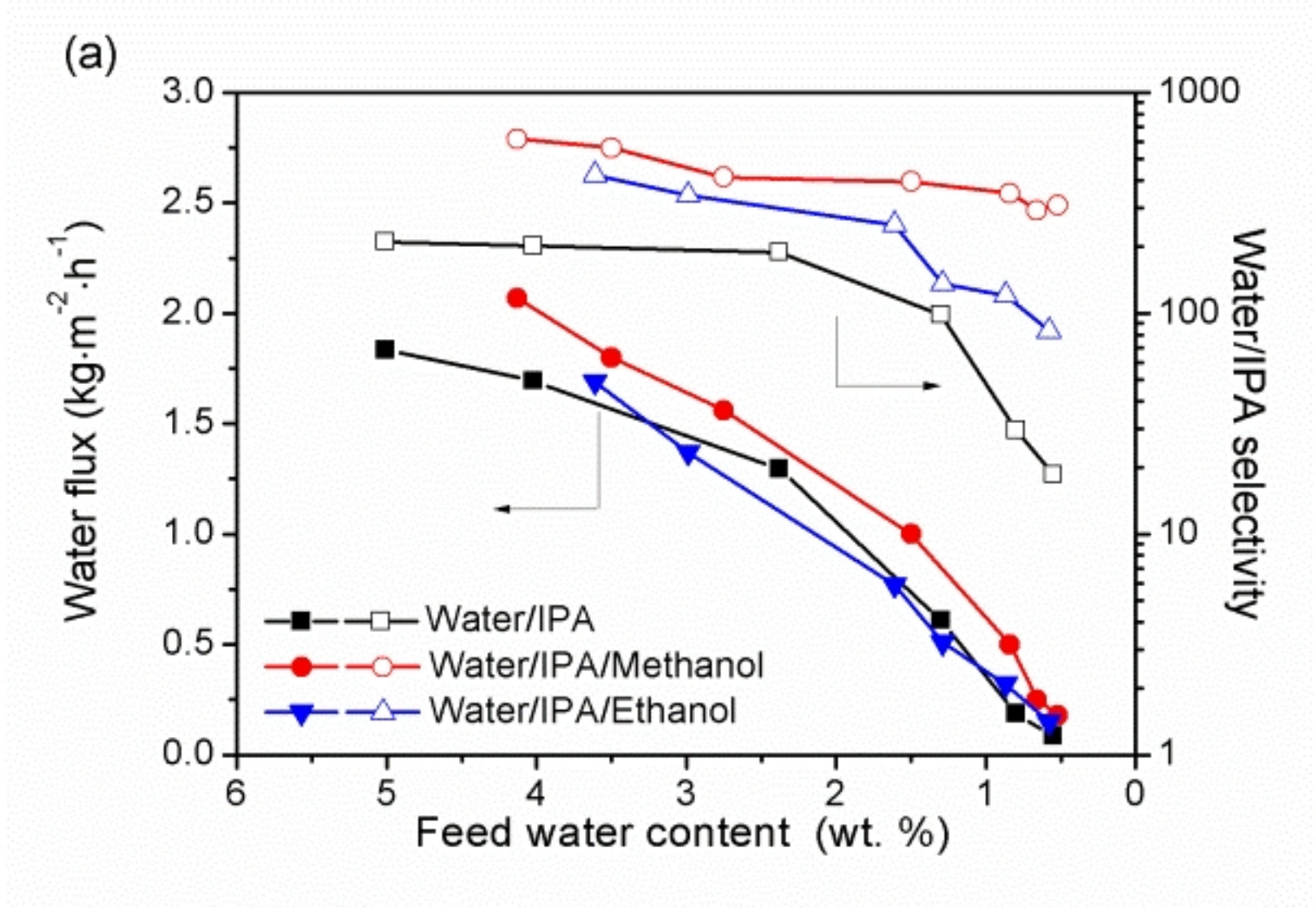
(a)
Water flux (kg·m-2·h-1)
Water/IPA selectivity
Feed water content (wt. %)
Water/IPA
Water/IPA/Methanol
Water/IPA/Ethanol
3.0
2.5
2.0
1.5
1.0
0.5
0.0
1000
100
10
1
6
5
4
3
2
1
0

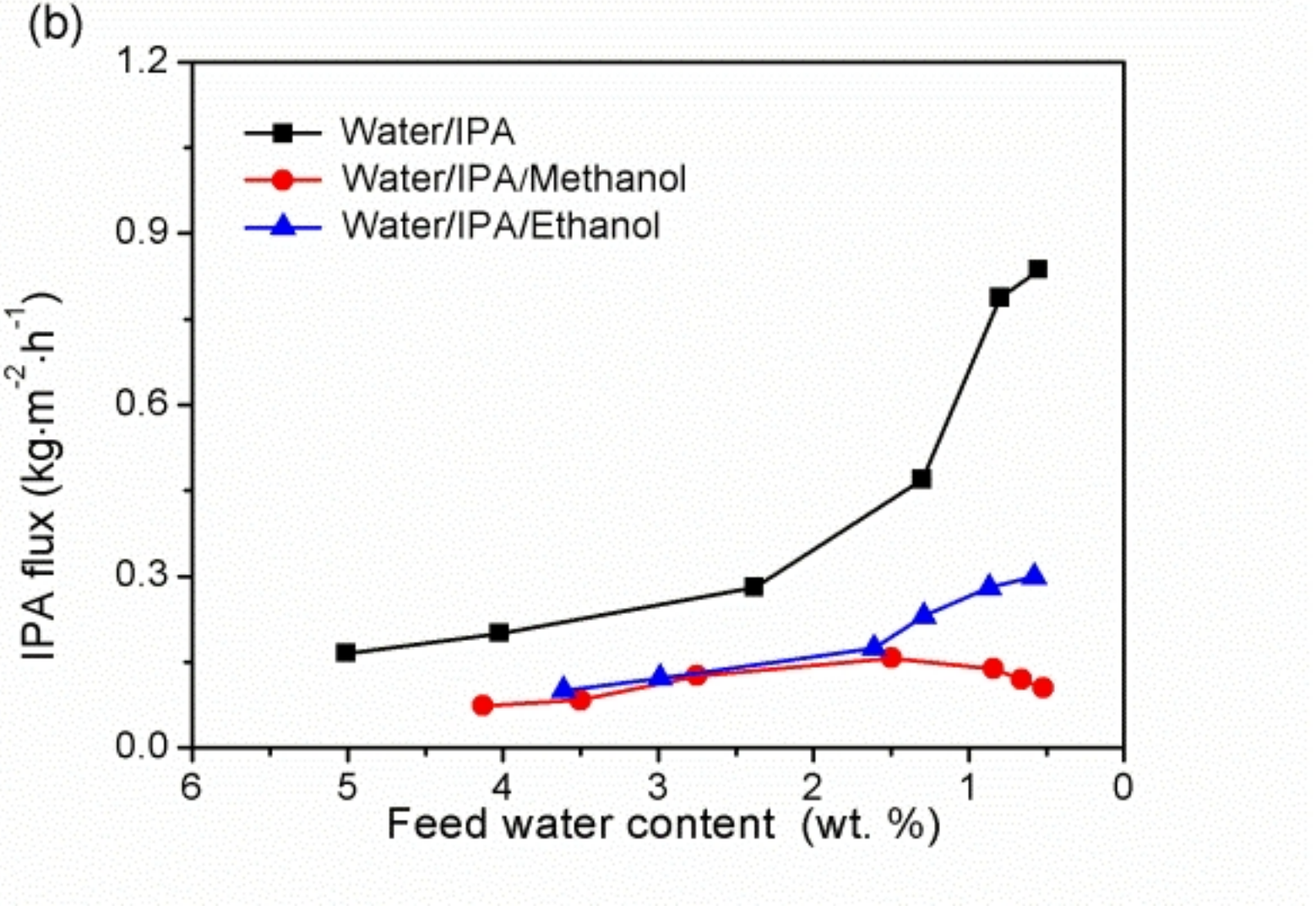
(b)
Water/IPA
Water/IPA/Methanol
Water/IPA/Ethanol
IPA flux (kg·m-2·h-1)
Feed water content (wt. %)
1.2
0.9
0.6
0.3
0.0
6
5
4
3
2
1
0

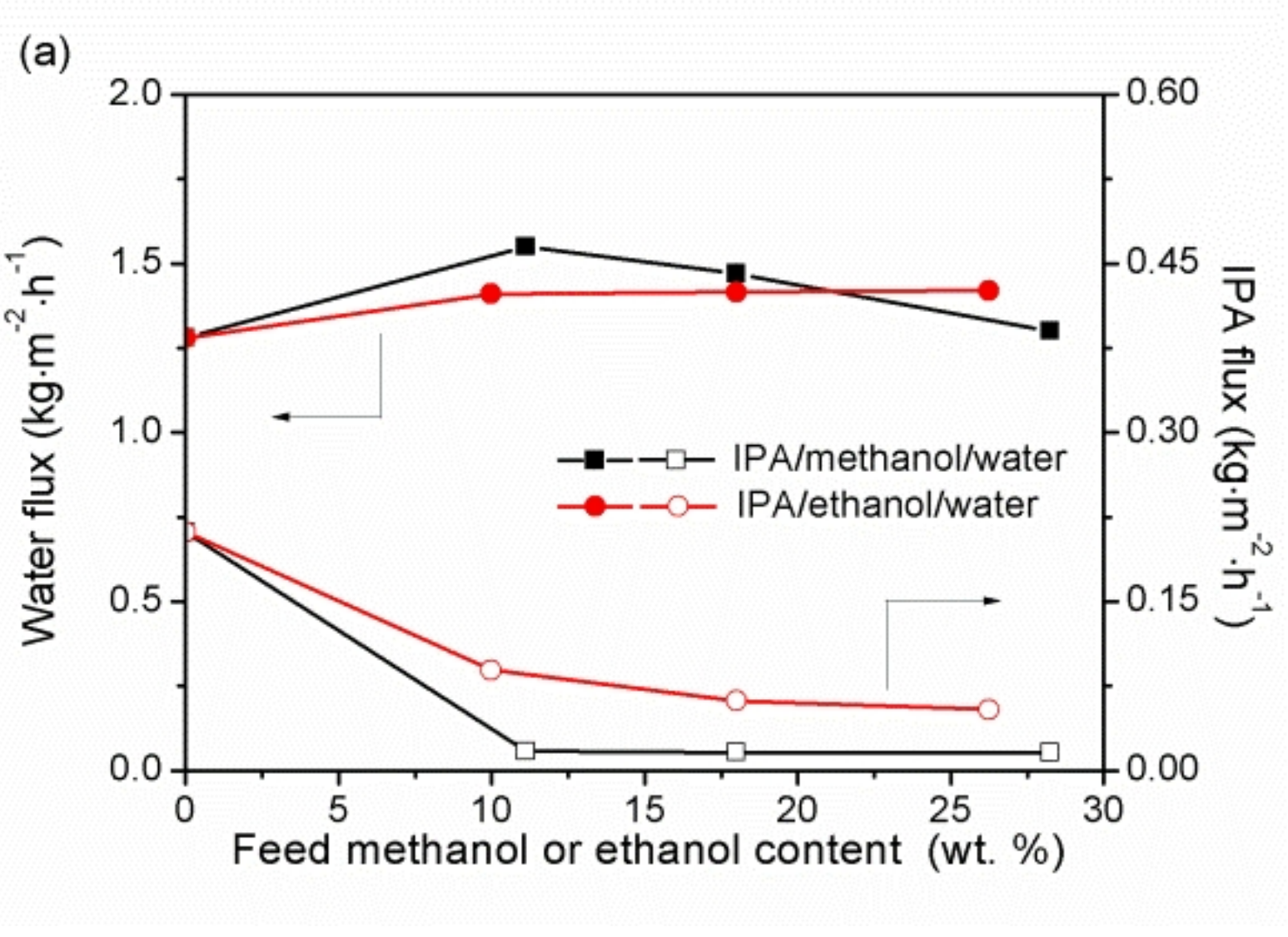
(a)
2.0
1.5
1.0
0.5
0.0
0.60
0.45
0.30
0.15
0.00
0
5
10
15
20
25
30
Water flux (kg·m-2·h-1)
IPA flux (kg·m-2·h-1)
Feed methanol or ethanol content (wt. %)
IPA/methanol/water
IPA/ethanol/water

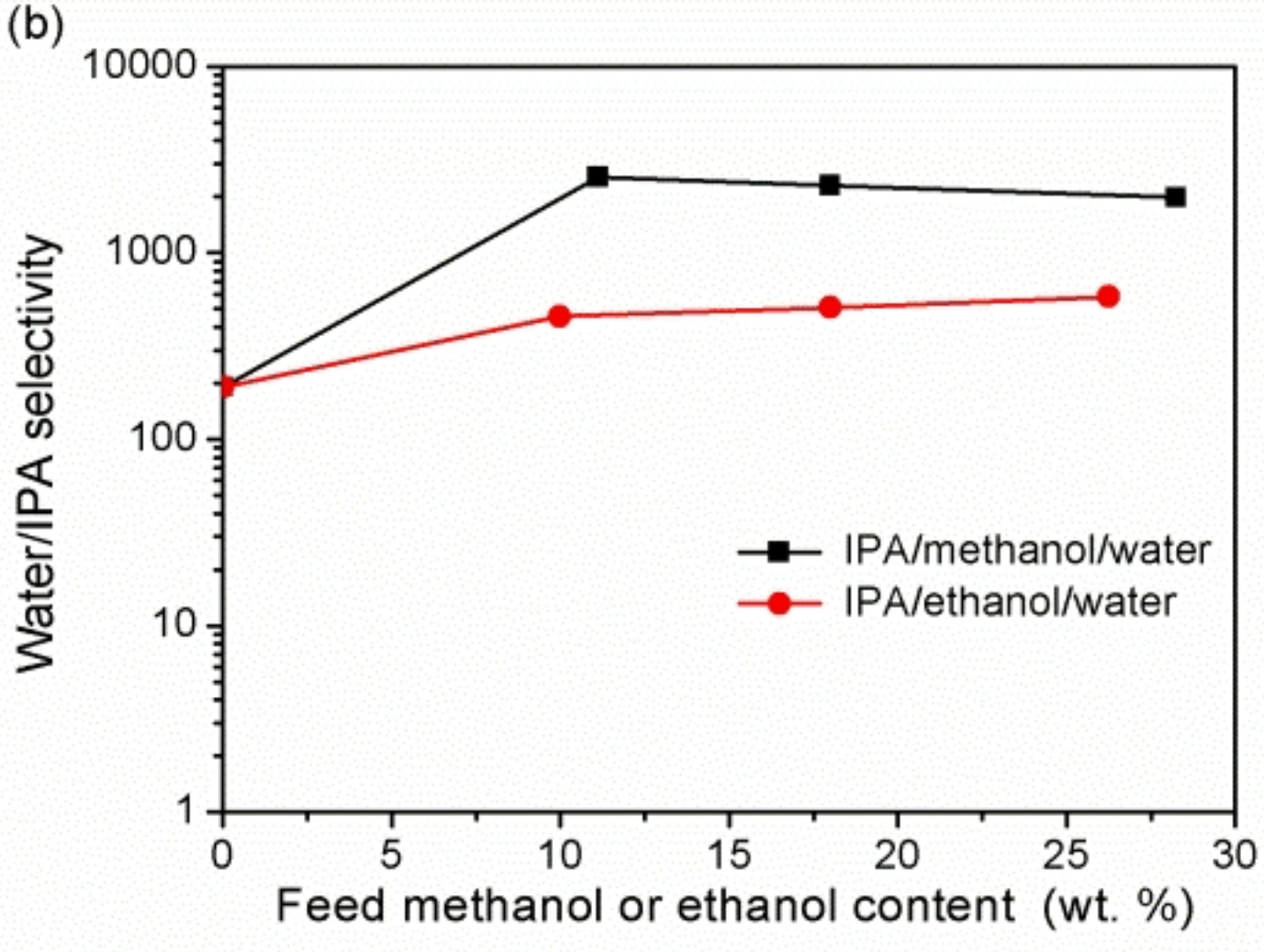
(b)
10000
1000
100
10
1
Water/IPA selectivity
0
5
10
15
20
25
30
Feed methanol or ethanol content (wt. %)
IPA/methanol/water
IPA/ethanol/water

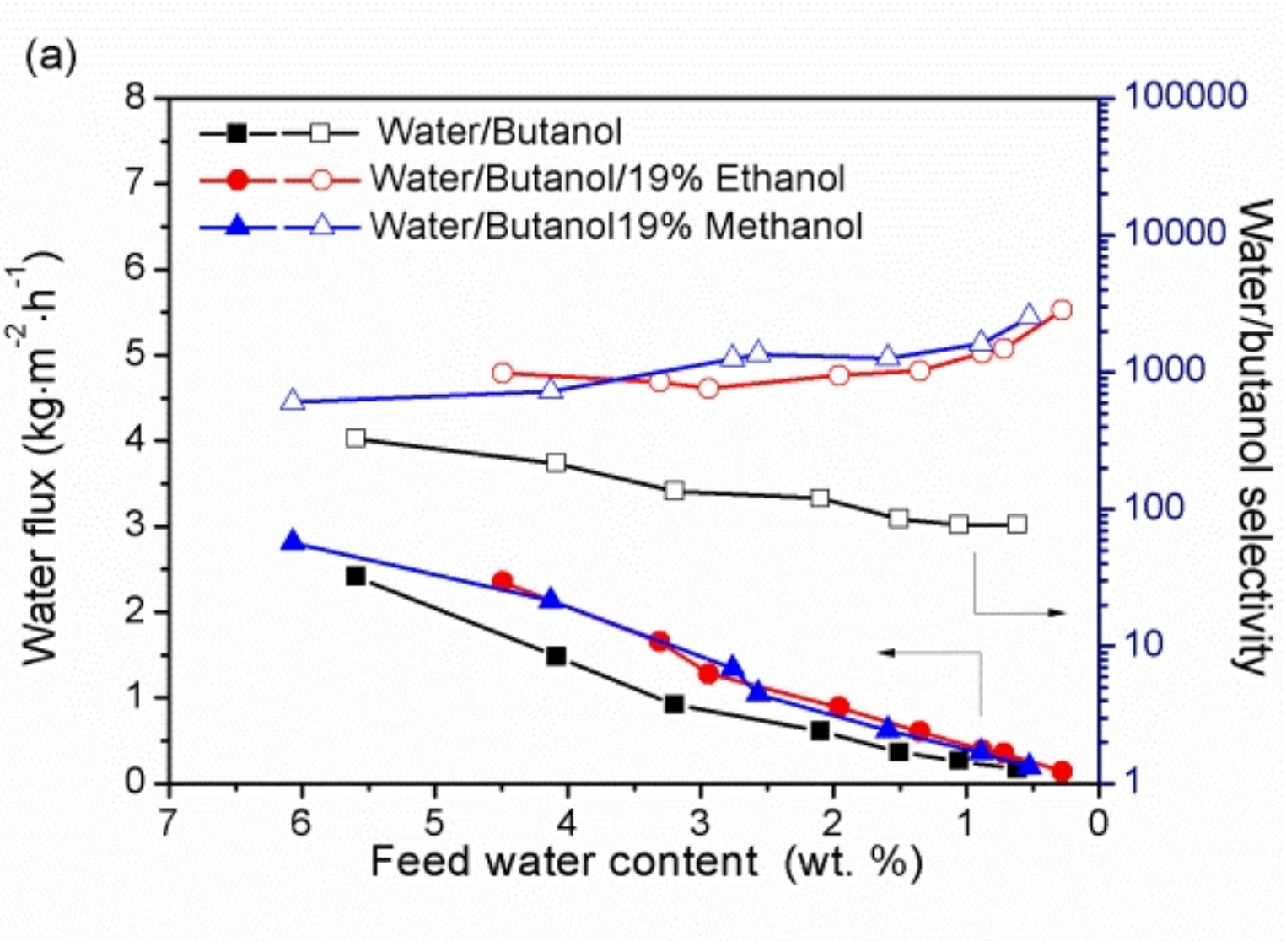
(a)
Water/Butanol
Water/Butanol/19% Ethanol
Water/Butanol19% Methanol
Water flux (kg·m-2·h-1)
Water/butanol selectivity
Feed water content (wt. %)
0
1
2
3
4
5
6
7
8
1
10
100
1000
10000
100000

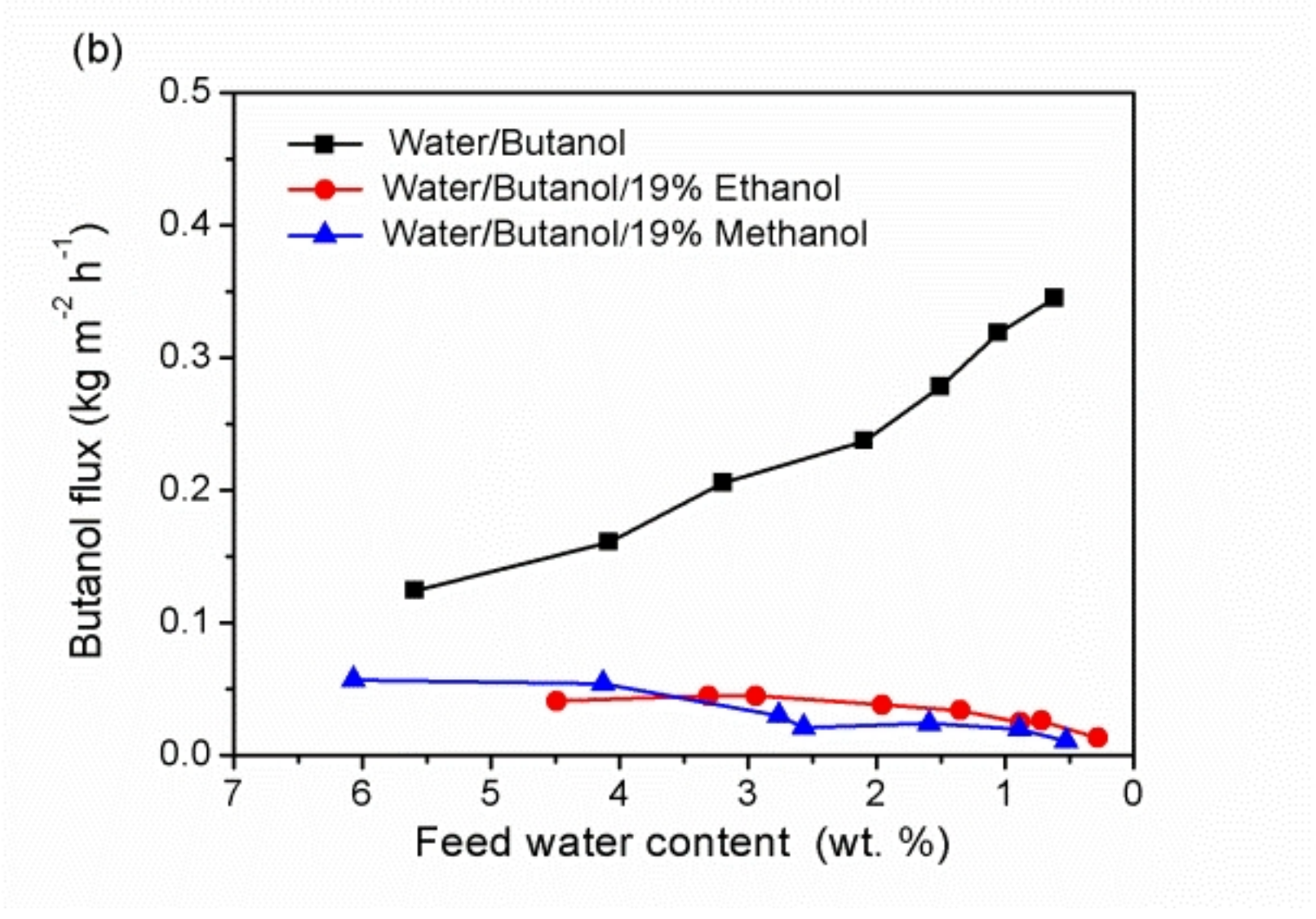
(b)
Water/Butanol
Water/Butanol/19% Ethanol
Water/Butanol/19% Methanol
Butanol flux (kg m-2 h-1)
0.0
0.1
0.2
0.3
0.4
0.5
7
6
5
4
3
2
1
0
Feed water content (wt. %)

- Expansion/contraction of NaA zeolite occurred at different water loadings.
- The adsorption-induced change influences on separation performance of NaA membrane.
- Methanol and ethanol can enter NaA zeolite pores to reduce the crystal contraction.